Interlayer RKKY interaction in ferromagnet/tilted Weyl semimetal/ferromagnet trilayer system

Yong-Jia Wu, Qing-Yun Xiong, Hou-Jian Duan,* Jia-Yan Ba, Ming-Xun Deng, and Rui-Qiang Wang†
Guangdong Provincial Key Laboratory of Quantum Engineering and Quantum Materials,
School of Physics and Telecommunication Engineering, South China Normal University, Guangzhou 510006, China

(Received 1 March 2022; accepted 31 October 2022; published 16 November 2022)

We have investigated the interlayer RKKY interaction in ferromagnet/Weyl semimetal/ferromagnet (FM/WSM/FM) trilayer system in the presence of the tilting effect of Weyl cones. Our investigation focuses on the influence of the unique features of WSMs: anisotropy dispersion, tilt effect, intervalley transitions, and Fermi arc states. Due to the separation of Weyl nodes, the RKKY behaviors, such as spin model, decaying rate, and oscillation period, heavily depend on the stacked direction of FMs, exhibiting strong magnetic anisotropy. Tilt of Weyl cones can increase the RKKY amplitude, change spin model, switch the antiferromagnetism and ferromagnetism, and more importantly generate the noncollinear Dzyaloshinskii-Moriya or spin-frustrated terms. Intervalley transition generates extra oscillation with period determined by separated distance between Weyl nodes, which together with Fermi-energy-induced oscillation leads to an interesting battering pattern. These signatures are significantly different from the interlayer RKKY interaction with single-node topological insulators or impurity RKKY case reported in previous literatures. More importantly, we find that the interlayer RKKY interaction decays more slowly with the spacer thickness than one reported extensively in WSMs doped with magnetic impurities, which is explained by providing a general formula. In addition, we discuss the effect from Weyl Fermi arcs. Compared to the bulk contributions, a more slowly decaying rate is found at the edges of ferromagnetic layer if the edges are parallel to the line connecting two Weyl nodes. Our research suggests that trilayer FM/WSM/FM is a more powerful platform to understand the WSM magnetic property and to extract the parameters of WSM materials by measuring the RKKY interaction.

DOI: 10.1103/PhysRevB.106.195130

I. INTRODUCTION

Weyl semimetals (WSMs), as one of the prominent members of topological material family, have been studied extensively due to their unique electronic band structure and potential applications in spintronics. The simplest low-energy model of WSMs can be described by two separated Weyl points with opposite chirality in momentum space. Each Weyl point corresponds to a magnetic or an antimagnetic monopole, which can be characterized by the nonzero Berry curvature. Due to the protection of the lattice-translation symmetry, the Weyl points can be created or annihilated only in pairs. Besides the chiral property, another fascinating feature for WSMs is the nontrivial Fermi arc [1,2], which connects the Weyl partners and contributes many novel transport phenomena [3–5]. WSMs can be realized from Dirac semimetals by breaking either the time-reversal or inversion symmetry [6–9], where a fourfold degenerate Dirac point is split into two Weyl points. So far, the WSMs with broken inversion symmetry have been extensively found in noncentrosymmetric transition-metal monosphides, e.g., TaP [10], NbP [11], NbAs [12], and TaAs [13–15]. Meanwhile, the WSMs with broken time-reversal symmetry have also been proposed in various magnetic materials, including $HgCr_2Se_4$, $Y_2Ir_2O_7$, $Co_3Sn_2S_2$, and Co_2-based Heusler compounds [16–20]. Very recently, $Co_3Sn_2S_2$ has already been experimentally verified to be a time-reversal broken WSM [21].

Besides the conventional WSMs with upright energy dispersions, a new type of tilted Weyl valleys with broken Lorentz invariance has recently been reported [22]. Considering the tilting effect in a certain axis, the WSMs can be divided into two categories by evaluating the ratio of the tilt parameter v_t and the Fermi velocity v_f. Specifically speaking, the valleys of type-I WSMs are only slightly tilted with $|v_t/v_f| < 1$, where the sign of the energy remains unchanged and the shapes of the Fermi surface at the Weyl points are pointlike. Differently, the valleys of type-II WSMs are flipped over as the tilting effect is strong enough with $|v_t/v_f| > 1$. In this scenario, a part of the energy in the conduction (valence) band becomes negative (positive) and the original pointlike Fermi surfaces are changed to be electron and hole pockets. Although the tilting effect does not change the topology of Weyl points, it significantly changes the shape of the Fermi surface, as well as the density of states (DOS) near the Fermi energy. Correspondingly, the tilting effect gives rise to many peculiar phenomena in the quantum transport, e.g., anomalous Nernst effect [23,24], planar Hall effect [25–27], magnetotransport [28,29], exotic Josephson effect in a Weyl superconductor junction [30], and specular Andreev reflection induced by the intraband electron-hole conversion [31,32]. Nevertheless, the magnetic properties with respect to the tilted WSMs has received little attention.

*dhjphd@163.com
†wangruiqiang@m.scnu.edu.cn

In the area of magnetic properties, the indirect exchange interaction, namely, the Ruderman-Kittel-Kasuya-Yosida (RKKY) interaction [33–35] mediated by the itinerant electrons of host materials, has attracted great interest in Dirac materials due to its potential applications in spin manipulation. One of the well-known examples is the anomalous Hall effect on the surface of the topological insulator [36,37], where nonzero net ferromagnetism can be induced by the Dzyaloshinskii-Moriya (DM) RKKY interaction. Besides manipulating the spins, the RKKY interaction has also been explored extensively to characterize the intrinsic properties of materials, including unique edge/surface states in topological materials [37–41], topological phase transitions [42], the nontrivial topology of the Fermi surface [43], the Rashba splitting [44], the spin-momentum locking [45,46], and so on. Notice that all the above literatures are focused on the RKKY interaction between magnetic impurities, whose signature is always difficult to be detected since the RKKY interaction decays fast with the increased impurity distance R. Interestingly, the study for the RKKY interaction was generalized to ferromagnet/spacer material/ferromagnet trilayer system, where the spacer was used with conventional metals such as Au or Cu in early works [47,48], and recently with topological insulator film [49,50] or Rashba semiconductors [51]. This seems to be an effective structure to generate the slowly decaying RKKY interaction. More importantly, this interlayer exchange coupling is not only an interesting phenomenon by itself, but also can be regarded as a probe to study the properties of the spacer, such as the topological phase or the tilting effect.

Motivated by this, we calculate the RKKY interaction between ferromagnetic layers in FM/WSM/FM trilayer system. We have studied the intervalley and intravalley contributions for tilted and untilted cases. The magnetic anisotropy of tilted WSMs has been revealed by considering different arrangements of the ferromagnetic layers. The qualitative differences exhibited by different stacking directions of the ferromagnetic layers highlight the role of the tilt in the magnetic trilayer geometry. In this way, various magnetic signatures characterizing the tilting effect are extracted. In addition, it is found that the interlayer RKKY interaction decays slowly with the spacer thickness $R_\perp$ as $R_\perp^{-2}$ ($R_\perp^{-3}$) for finite (zero) Fermi energy u_F. It is significantly different from the RKKY interaction of magnetic impurities in WSMs [45,46,52], which decays fast with the impurity distance R as R^{-3} (R^{-5}) for $u_F \neq 0$ ($u_F = 0$). Through this paper, trilayer systems are suggested as more powerful platforms to characterize the intrinsic properties of materials, superior to extensively adopted systems doping with magnetic impurities.

The paper is organized as follows. In Sec. II, we introduce a low-energy model of tilted WSM and show the method for calculating the interlayer RKKY interaction in FM/WSM/FM trilayer system. The results of the interlayer interaction in WSM with different arrangements of FMs have been discussed in Secs. III A–III C, which consist of intravalley and intervalley contributions. The cases of the tilted and untilted valleys, as well as the finite and zero Fermi energies, are also discussed. In Sec. III D we further explore the origin of the slow-decaying law of the interlayer RKKY interaction. In Sec. III E, the contribution from the Fermi arc to the interlayer RKKY interaction is discussed. Finally, a short summary is given in Sec. IV.

II. MODEL AND METHOD

We start with a minimal low-energy model of tilted magnetic WSMs, whose Hamiltonian is [53]

$$H_{\text{Weyl}} = v_f(k_x\sigma_x + k_y\sigma_y) + \lambda v_f(k_z - \lambda Q)\sigma_z + v_t k_y, \quad (1)$$

where $\sigma_{x,y,z}$ are Pauli matrices acting on the real spin space. The first two terms in the above equation describe a WSM with broken time-reversal symmetry, whose dispersion is composed of two Weyl points splitting along z axis, respectively, located at $(0, 0, \lambda Q)$ with opposite chirality $\lambda = \pm$. The last term introduces the tilting effect of linear dispersion assumed to along k_y axis, and the ratio of $|v_t/v_f|$ evaluates the extent of the tilt. Here, we only consider the type-I WSM with $|v_t/v_f| < 1$ and set $v_t > 0$. By diagonalizing the Hamiltonian H, the eigenvalues can be easily solved as

$$E_{s,\lambda} = v_t k_y + s\varepsilon_\lambda(\mathbf{k}), \quad (2)$$

with $\varepsilon_\lambda(\mathbf{k}) = v_f\sqrt{k_x^2 + k_y^2 + (k_z - \lambda Q)^2}$. The corresponding eigenfunction reads as

$$\Psi_{s,\lambda}(\mathbf{k}) = \frac{1}{\sqrt{2\varepsilon_\lambda[\varepsilon_\lambda + s\lambda v_f(k_z - \lambda Q)]}} \times \begin{pmatrix} s\varepsilon_\lambda + \lambda v_f(k_z - \lambda Q) \\ v_f(k_x + ik_y) \end{pmatrix}, \quad (3)$$

where $s = \pm$ represent the conduction and valence bands. Notice that the tilting parameter v_t does not affect the eigenfunctions and only enters into the band energies by tilting the Weyl valleys.

In this paper, we consider a system with sandwiched structure, where two ferromagnet metals (e.g., Fe, Co, Gd, and their compounds [47,48,54,55]) are respectively placed on the top (F^T) and bottom (F^B) of the structure, and a WSM acts as the spacer material, as shown in Fig. 1. The distance between two ferromagnets is $R_\perp = (N + 1)a$, where a is the thickness of unit cell of WSM along its stacking direction and N is an integer. The plane of the ferromagnetic layer adjacent to WSM is assumed to be fully filled with classical spins $\mathbf{S}_i$. The spin exchange interaction $H_{\text{int}} = J_0\delta(\mathbf{r} - \mathbf{R}_i)\mathbf{s}\cdot\mathbf{S}_i$ describes a direct coupling between $\mathbf{S}_i$ (located at the atomic position $\mathbf{R}_i$) and the spins $\mathbf{s}$ of itinerant electrons of the WSM spacer, where J_0 is the coupling strength. For the case of weak coupling J_0, H_{int} can be regarded as a perturbation. Under the standard perturbation theory, the indirect interlayer RKKY interaction between ferromagnetic layers can be expressed as [47,48,51]

$$J(R_\perp) = -\sum_{\alpha,\beta=x,y,z} \frac{J_0^2 S_\alpha^T S_\beta^B a}{2(2\pi)^3 V_0} \int_{-\pi/a}^{\pi/a} dq_\perp e^{iq_\perp R_\perp} \times \int_{2DBZ} d\mathbf{q}_\parallel \chi_{\alpha\beta}(\mathbf{q}_\parallel, q_\perp) \sum_{\mathbf{R}_\parallel \in F^T} e^{i\mathbf{q}_\parallel\cdot\mathbf{R}_\parallel}, \quad (4)$$

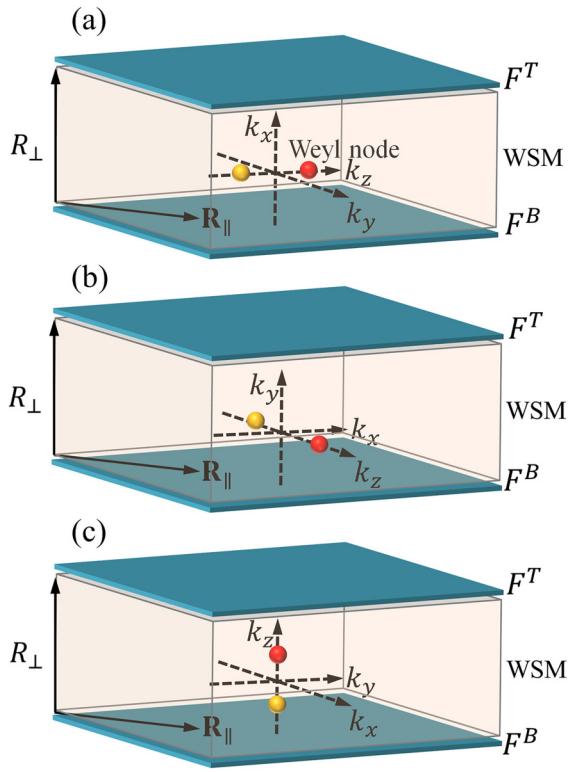

FIG. 1. Schematic diagram for a trilayer structure with two ferromagnets F^T and F^B placed on the top and bottom, respectively, and a WSM acts as the spacer material. Different stacking directions of the ferromagnetic layers are considered as: (a) $R_\perp = R_x$, $\mathbf{R}_\parallel = (R_y, R_z)$; (b) $R_\perp = R_y$, $\mathbf{R}_\parallel = (R_z, R_x)$; (c) $R_\perp = R_z$, $\mathbf{R}_\parallel = (R_x, R_y)$.

where V_0 is the volume of the unit cell, $S_\alpha^T (S_\beta^B)$ is the spin of the top (bottom) ferromagnetic layer, $\chi_{\alpha\beta}(\mathbf{q}_\parallel, q_\perp)$ describes the static spin susceptibility tensor with the subscript $\perp$ ($\parallel$) representing the direction perpendicular (parallel) to the plane of ferromagnetic layers. The electrons of the WSM participating in the exchange coupling enter into the $\chi_{\alpha\beta}(\mathbf{q}_\parallel, q_\perp)$ term, and are finally reflected in $J(R_\perp)$, from which we can extract the information of the properties of WSMs.

The planar dimensions of the ferromagnetic layers satisfy the periodic boundary conditions since they are assumed to be large as compared to the spacer thickness $R_\perp$. Considering this periodic boundary condition and performing the integration of $\mathbf{q}$ within the first Brillouin zone, the effective $\mathbf{q}_\parallel$ in Eq. (4) must satisfy [47,48,51] $\mathbf{q}_\parallel = 0$, otherwise the summation $\sum_{\mathbf{R}_\parallel \in F^T} e^{i\mathbf{q}_\parallel \cdot \mathbf{R}_\parallel}$ is zero for $\mathbf{q}_\parallel \neq 0$. In addition, when the calculation is performed within the low-energy regime, where the largest Fermi wave numbers in all directions are much smaller than π/a, the integral range $(-\pi/a, \pi/a)$ of $q_\perp$ in Eq. (4) can be replaced with $(-\infty, \infty)$. In this way, the interlayer RKKY interaction $J(R_\perp)$ of Eq. (4) can be further simplified as

$$J(R_\perp) = -\sum_{\alpha,\beta=x,y,z} \frac{S_\alpha^T S_\beta^B J_0^2 a^2}{4\pi V_0^2} \int_{-\infty}^{\infty} dq_\perp e^{iq_\perp R_\perp} \chi_{\alpha\beta}(0, q_\perp), \tag{5}$$

and the static spin susceptibility $\chi_{\alpha\beta}$ can be calculated through

$$\chi_{\alpha\beta}(0, q_\perp) = -\frac{\mu_B^2}{\gamma} \sum_{ik_n, \mathbf{k}} \sum_{\lambda,\lambda'} \times \mathrm{Tr}\left[G^{\lambda}_{k_\perp, \mathbf{k}_\parallel}(ik_n)\sigma_\alpha G^{\lambda'}_{k_\perp + q_\perp, \mathbf{k}_\parallel}(ik_n)\sigma_\beta\right], \tag{6}$$

where $\mathbf{k} = (k_\perp, \mathbf{k}_\parallel)$, $\gamma = 1/(k_B T)$, μ_B is the Bohr magneton, and k_n is the fermionic Matsubara frequency.

In calculating the static spin susceptibility $\chi_{\alpha\beta}$, we should obtain the Matsubara Green's function $G_{\mathbf{k}}(ik_n)$, which is constructed by using the eigenvalues and eigenfunctions in Eqs. (2) and (3), and given by

$$G^{\lambda}_{k_\perp, \mathbf{k}_\parallel}(ik_n) = \sum_{s=\pm} \frac{\Psi_{s,\lambda}(\mathbf{k})\Psi^\dagger_{s,\lambda}(\mathbf{k})}{ik_n + u_F - E_{s,\lambda}} = \frac{ik_n + u_F - v_t k_y + H_0(\mathbf{k})}{(ik_n + u_F - v_t k_y)^2 - \varepsilon^2_{\lambda,\mathbf{k}}}, \tag{7}$$

where $H_0(\mathbf{k})$ is the Hamiltonian of nontilted WSMs. The concrete form of $(k_\perp, \mathbf{k}_\parallel)$ depends on the stacking direction of the ferromagnetic layers. Specifically, if the ferromagnetic layers F^T and F^B are stacked along l axis, the corresponding components of $(k_\perp, \mathbf{k}_\parallel)$ are $k_\perp = k_l$ and $\mathbf{k}_\parallel = (k_m, k_n)$ with $l, m, n = x, y, z$ $(l \neq m \neq n)$. Due to the anisotropy of the WSMs with tilted dispersion, the interlayer RKKY interaction for different arrangements of the ferromagnetic layers will be discussed in the next section.

Notice that an energy gap would be opened at the Weyl points due to the quantum confinement effect, when the WSM film is thin enough. As reported in recent work [56,57], the critical thickness of the film for maintaining the gapless WSM state is at least 10 nm. To avoid destroying the Weyl points in this paper, the interlayer RKKY interaction is discussed with a safe range of the thickness $R_\perp$, i.e., $R_\perp Q > 10$ with the model parameter [58] $Q = 0.9\ \mathrm{nm}^{-1}$.

III. RESULTS AND DISCUSSION

A. Interlayer RKKY interaction with FMs stacked in the *x* axis

In this section, we consider the interlayer RKKY interaction mediated by the WSM with two FMs stacked along the x axis [Fig. 1(a)], i.e., $k_\perp = k_x$ and $\mathbf{k}_\parallel = (k_y, k_z)$. Substituting Eq. (7) to Eq. (6), the static spin susceptibility $\chi_{\alpha\beta}(0, q_x)$ can be simplified as

$$\chi_{\alpha\beta}(0, q_x) = \frac{-\mu_B^2}{\gamma} \sum_{\lambda, k_n, \mathbf{k}} \frac{\mathrm{Tr}\{[ik_n + u_F - v_t k_y + H_0(\mathbf{k})]\sigma_\alpha [ik_n + u_F - v_t k_y + H_0(k_x + q_x, \mathbf{k}_\parallel)]\sigma_\beta\}}{\left[(k_n - iu_F + iv_t k_y)^2 + \varepsilon^2_\lambda(\mathbf{k})\right]\left[(k_n - iu_F + iv_t k_y)^2 + \varepsilon^2_\lambda(k_x + q_x, \mathbf{k}_\parallel)\right]}, \tag{8}$$

where $\mathbf{k} = (k_x, \mathbf{k}_\parallel)$. Noting that all contributions to $\chi_{\alpha\beta}(0, q_x)$ stem from the intravalley process, i.e., $\lambda' = \lambda$ in Eq. (6), while the intervalley one has no effect in this arrangement. The reason is that the projections of two Weyl valleys in the k_x axis are

completely overlapped. To avoid the divergent integrals in the Eq. (8), one can use the following Feynman parametrization [59]:

$$\frac{1}{(k_n - iu_F + iv_t k_y)^2 + \varepsilon_\lambda^2(\mathbf{k})} \cdot \frac{1}{(k_n - iu_F + iv_t k_y)^2 + \varepsilon_\lambda^2(k_x + q_x, \mathbf{k}_\parallel)} = \int_0^1 dg \frac{1}{\left[(k_n - iu_F + iv_t k_y)^2 + \varepsilon_\lambda^2(\mathbf{k}) + g q_x v_f^2 (2k_x + q_x)\right]^2}. \tag{9}$$

In this way, the static spin susceptibility $\chi_{\alpha\beta}(0, q_x)$ can be expressed as

$$\chi_{\alpha\beta}(0, q_x) = \frac{-\mu_B^2}{(2\pi)^4} \sum_\lambda \int dk_n \int d\mathbf{k} \int_0^1 dg \frac{\mathrm{Tr}\{[ik_n + u_F - v_t k_y + H_0(k_x, \mathbf{k}_\parallel)]\sigma_\alpha [ik_n + u_F - v_t k_y + H_0(k_x + q_x, \mathbf{k}_\parallel)]\sigma_\beta\}}{\left[(k_n - u_F + iv_t k_y)^2 + \varepsilon_\lambda^2(k_x, \mathbf{k}_\parallel) + g q_x v_f^2 (2k_x + q_x)\right]^2}. \tag{10}$$

Using the coordinate transformation $(k_x + g q_x, k_z - \lambda Q) = (k_x', k_z')$, the above equation can be further simplified as

$$\chi_{\alpha\beta}(0, q_x) = \frac{-\mu_B^2}{(2\pi)^4} \sum_\lambda \int dk_n \int d\mathbf{k}' \int_0^1 dg \frac{\mathrm{Tr}\{[ik_n + u_F - v_f g q_x \sigma_x + h(\mathbf{k}')]\sigma_\alpha [ik_n + u_F + v_f q_x (1-g)\sigma_x + h(\mathbf{k}')]\sigma_\beta\}}{\left[(k_n - iu_F + iv_t k_y)^2 + v_f^2 |\mathbf{k}'|^2 + g(1-g) v_f^2 q_x^2\right]^2}, \tag{11}$$

with

$$h(\mathbf{k}') = -v_t k_y + v_f (k_x' \sigma_x + k_y \sigma_y + \lambda k_z' \sigma_z). \tag{12}$$

Plugging $\chi_{\alpha\beta}(0, q_x)$ into Eq. (5) and tracing over the Pauli matrices, the interlayer RKKY interaction $J(R_x)$ can be expressed in the following form:

$$J(R_x) = \sum_{\alpha=x,y,z} J_\alpha(R_x) S_\alpha^T S_\alpha^B + J_x^{DM}(R_x)(\mathbf{S}^T \times \mathbf{S}^B)_x, \tag{13}$$

where $J_\alpha(R_x)$ couples collinear spins and $J_x^{DM}(R_x)$ describes the DM (noncollinear) interaction, which has been revealed to twist the spin orientations of neighboring spins and regarded as an origin of the anomalous Hall effect on the surface of three-dimensional topological insulators [36,37].

First, we discuss the case of $u_F = 0$, which can let us to obtain analytical expressions. After some algebraic calculations (see Appendix A), the analytical results of the interlayer RKKY components can be obtained as

$$\begin{aligned} J_{y,z}(R_x, u_F = 0) &= -\frac{4\pi^3 J_c}{3 v_f} \frac{1}{R_x^3}, \\ J_x(R_x, u_F = 0) &= 0, \\ J_{x,y,z}^{DM}(R_x, u_F = 0) &= 0, \end{aligned} \tag{14}$$

with $J_c = J_0^2 \mu_B^2 a^2 / (16\pi^5 V_0^2)$. As shown above, the DM interaction vanishes, and there only exists in-plane collinear components, exhibiting the XYY spin model for the interlayer RKKY interaction. Notice that the vanished out-of-plane collinear component $J_x(R_x)$ is attributed to the suppressed intravalley contribution by the two-dimensional structure of the ferromagnetic layers, which distinguishes from the nonzero out-of-plane RKKY component between zero-dimensional magnetic impurities in WSMs [45,46]. In addition, the tilting effect does not affect the interlayer RKKY interaction at zero Fermi energy $u_F = 0$ since the interaction is determined by the energy difference [51] $E_{+,\lambda}(k_x, k_\parallel) - E_{-,\lambda}(k_x + q_x, k_\parallel)$, independent on the parameter v_t for $u_F = 0$.

For $u_F \neq 0$ and $v_t = 0$, all the interlayer RKKY components have to be calculated numerically according to Eqs. (5) and (11)–(13), and we plot the numerical results in Fig. 3. Compared to the case of $u_F = 0$, there are three main differences: (i) Except for the vanished $J_x(R_x)$, the other components $J_{y/z}(R_x)$ and $J_x^{DM}(R_x)$ are nonzero. They exhibit an oscillating behavior with the period of π/k^0, where $k^0 = u_F/v_f$ corresponds to the isotropic Fermi wave number. The oscillation of the RKKY interaction is induced by the Kohn anomaly [51], which corresponds to the singular point on the Fermi surface, whose projection is denoted in Fig. 2(b); (ii) The original fast-decaying interlayer components [R_x^{-3} in Eq. (14)] are prolonged as R_x^{-2}; (iii) The amplitude of the nonzero interlayer RKKY components exhibit a linear relation with the Fermi energy, i.e., $J_{y/z}, J_x^{DM} \propto u_F$, as shown in Fig. 3(b). In Fig. 3, The numerical results for the nonzero

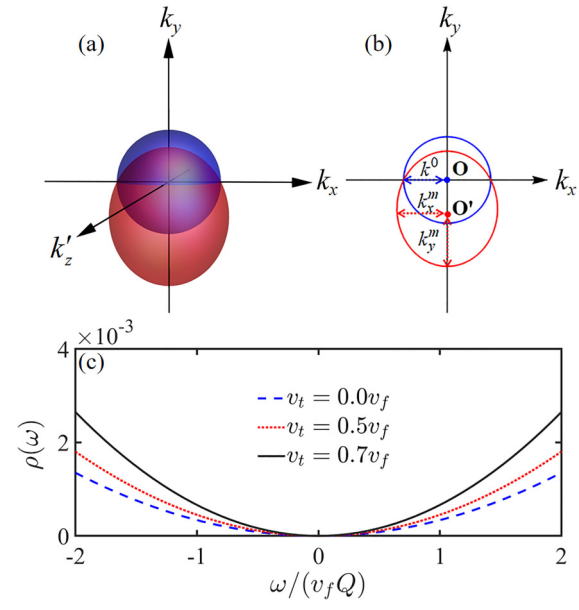

FIG. 2. (a) The three-dimensional Fermi surfaces and (b) the edge of its projection on the $k_x - k_y$ plane for $v_t = 0$ (blue color) and $v_t \neq 0$ (red color). Only one Weyl valley ($k_z' = k_z - \lambda Q$ for $\lambda = +$ or $-$) with finite Fermi energy is considered since the other one shares the same response to the tilting term $v_t k_y$. (c) The energy-dependent DOS for different v_t.

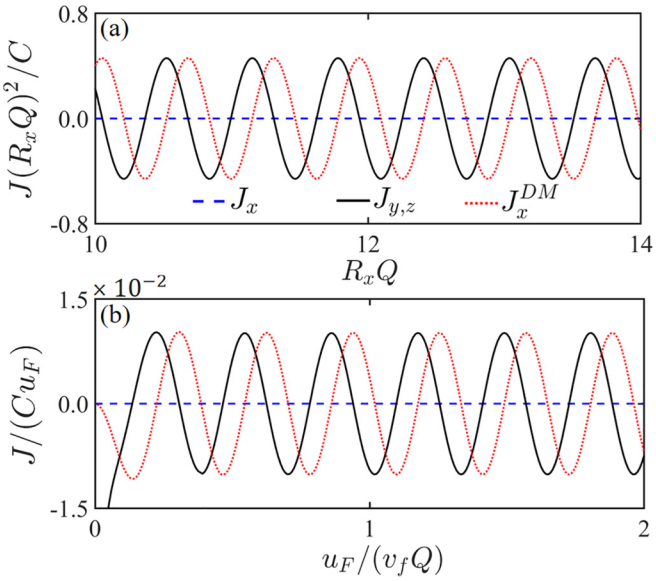

FIG. 3. Dependence of the interlayer RKKY components on (a) the spacer thickness R_x and (b) the Fermi energy u_F. The period of the oscillation in (a) is π/k^0. Other parameters are set as: $C = J_0^2\mu_B^2a^2/(32\pi^5V_0^2v_f^4)$, $u_F = 5v_fQ$ in (a) and $R_xQ = 10$ in (b).

interlayer RKKY components of $u_F \neq 0$ can be fit in the following function:

$$J_\alpha(R_x, u_F \neq 0) \propto \frac{u_F}{R_x^2}\sin(2k_0R_x + \eta), \tag{15}$$

where η is a constant. Interestingly, the interlayer RKKY interaction here decays much more slowly than the RKKY interaction of magnetic impurities in WSMs [45,46,52], where the interaction decays fast with the impurity distance R as R^{-3} (R^{-5}) for $u_F \neq 0$ ($u_F = 0$). The slowly decaying law in Eqs. (14) and (15) means that the trilayer structure can prolong the decay of the RKKY interaction and make it easier to detect the magnetic signals characterizing the intrinsic properties of spacer materials.

For $u_F \neq 0$ and $v_t \neq 0$, the tilt-modified interlayer RKKY interaction can be calculated numerically according to Eqs. (5) and (11)–(13). As shown in Fig. 4, the cases with and without tilting effect are compared. The original $J_y = J_z$ for $v_t = 0$ is changed to be $J_y \neq J_z$ by finite v_t (except for some special values of vanished $J_{y,z}$). The underlying physics is attributed to the broken rotational symmetry around the k_x axis by the tilting effect of k_y axis. Obviously, the tilting effect does not change the decay of the interaction since the exponent ζ of the DOS of WSMs can not be disturbed by nonzero v_t .

Another main modification in Fig. 4 induced by the tilt is that the oscillation period is decreased with the increased tilting parameter v_t . This is attributed to the deformation of the Fermi surface. Specifically speaking, when v_t varies from zero to a finite value, the original spherical Fermi surface is transformed into an ellipsoidal one, as shown in Figs. 2(a). This deformation leads to the shift of the position of the Kohn anomaly, whose projection in the stacking direction (k_x axis) is also changed from k^0 to k_x^m, i.e., the short axis of the ellipse in Fig. 2(b). When the transferred momentum $q_\perp = q_x$ is integrated out in Eq. (5), k_x^m would enter into the

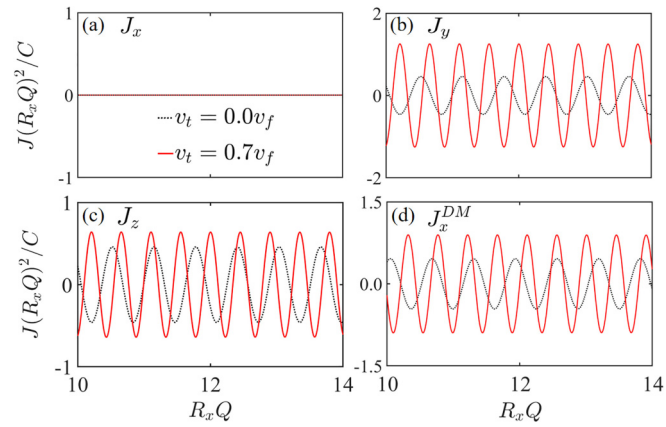

FIG. 4. The interlayer RKKY components versus the spacer thickness R_x for tilted and untilted cases. The period of the oscillation is $\pi\sqrt{v_f^2 - v_t^2}/u_F$. Other parameters are the same as Fig. 3(a).

phase factor $e^{i2k_x^mR_x}$ to display periodic functions $\sin(2k_x^mR_x)$ or $\cos(2k_x^mR_x)$. According to the properties of singular point, one can use the partial differential equations of $\partial k_x/\partial k_{y,z} = 0$ $[k_x = \pm\sqrt{(u_F - v_tk_y)^2/v_f^2 - k_y^2 - k_z^2}]$ to calculate k_x^m, which is solved as $k_x^m = u_F/\sqrt{v_f^2 - v_t^2}$. The corresponding period of the oscillation of the interaction is

$$T' = \pi/k_x^m = \pi\sqrt{v_f^2 - v_t^2}/u_F, \tag{16}$$

which explains the oscillation period shown in Fig. 4. Importantly, from this simply oscillation period, we can easy to extract the tilt parameter v_t. Since v_t enters into the periodic function $\sin(2k_x^mR_x)$ or $\cos(2k_x^mR_x)$, the magnetism of the interaction would be changed when v_t varies. As shown in Fig. 5, all the finite RKKY components would be changed between antiferromagnetism and ferromagnetism. In addition, the amplitude of all the nonzero RKKY components increases with v_t. This can be understood by checking the DOS $\rho(\omega) = \rho_0(\omega)/(1 - v_t^2/v_f^2)^2$ where $\rho_0(\omega) = \omega^2/(2\pi^2v_f^3)$ is the DOS of untilted WSMs. As shown in Fig. 2(c), when v_t increases, the DOS would be enhanced correspondingly. Notice that the magnetic indirect exchange interaction is mainly mediated by the itinerant electrons near the Fermi surface. Large tilt means that more electrons are allowed to participate in the scattering between ferromagnetic layers and so enhance the amplitude of the RKKY interaction.

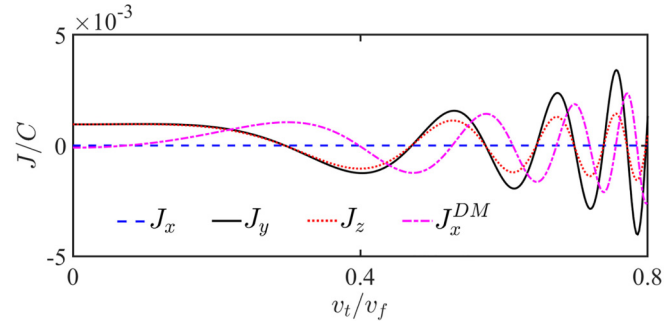

FIG. 5. v_t-dependent interlayer RKKY components with $R_xQ = 12$ and $u_F = 1.5v_fQ$.

B. Interlayer RKKY interaction with FMs stacked in *y* axis

For the arrangement of FMs with their stacking direction parallel to the y axis [i.e., tilted direction, see Fig. 1(b)], $q_\perp = q_y$, $k_\perp = k_y$ and $\mathbf{k}_\parallel = (k_z, k_x)$. Similar to the case with ferromagnetic layers stacked in the x axis, the interlayer RKKY interaction here is only contributed by the intravalley coupling, i.e., $\lambda = \lambda'$. Following the similar procedure, one can use the Eqs. (5)–(7) to simplify the interlayer RKKY interaction $J(R_y)$ as

$$J(R_y) = \sum_{\alpha=x,y,z} J_\alpha(R_y) S_\alpha^T S_\alpha^B + J_y^{DM}(R_y)(\mathbf{S}^T \times \mathbf{S}^B)_y. \quad (17)$$

For $v_t = 0$, the results of $J_\alpha(R_y)$ [$J_y^{DM}(R_y)$] can be easily obtained by simply rotating the direction of the RKKY components $J_\alpha(R_x)$ [$J_x^{DM}(R_x)$] around the z axis by 90 degrees clockwise, i.e., $J_x(R_y) = J_y(R_x)|_{R_x\to R_y}$, $J_y(R_y) = -J_x(R_x)|_{R_x\to R_y}$, $J_z(R_y) = J_z(R_x)|_{R_x\to R_y}$ and $J_y^{DM}(R_y) = -J_x^{DM}(R_x)|_{R_x\to R_y}$. This is a reflection of the rotational symmetry of the energy dispersion around the k_z axis.

For $u_F = 0$ and $v_t \neq 0$, the analytical expressions of $J(R_y)$ can be obtained after some algebraic calculations (see Appendix B), given by

$$\begin{aligned} J_{x,z}(R_y, u_F = 0) &= -\frac{4\pi^3 J_c}{3v_f}\frac{(1 - v_t^2/v_f^2)}{R_y^3}, \\ J_y(R_y, u_F = 0) &= \frac{4\pi^3 J_c}{3v_f^3}\frac{v_t^2}{R_y^3}, \\ J_y^{DM}(R_y, u_F = 0) &= 0. \end{aligned} \quad (18)$$

Different from the case of FMs stacked in x axis, here the interlayer RKKY interaction can be modified by the valley tilt even for zero Fermi energy. The variation of the interaction increases parabolically with v_t in the form of $J_\alpha(v_t \neq 0) - J_\alpha(v_t = 0) \propto v_t^2/R_y^3$. This is attributed to the tilt-dependent energy difference [51] $E_{+,\lambda}(k_y, k_\parallel) - E_{-,\lambda}(k_y + q_y, k_\parallel)$ [see Eq. (2)], where the transferred momentum q_y couples tightly with v_t. Still, the collinear components exhibit a XXY spin model and the DM interaction vanishes even in the presence of the tilting effect.

For $u_F \neq 0$ and $v_t \neq 0$, the numerical results (not shown) of $J(R_y, u_F \neq 0)$ here are similar to the case in Sec. III A, including the interaction with tilt-independent prolonged decaying rate [$J(R_y, u_F \neq 0) \propto R_y^{-2}$], the similar tilt-modified oscillation function $\sin(2k_y^m R_y)$ for $J(R_y, u_F \neq 0)$ with $k_y^m = u_F v_f/(v_f^2 - v_t^2)$ being the largest Fermi wave number in the stacking direction [Fig. 2(b)], and the magnetism switching induced by the tilting parameter v_t.

C. Interlayer RKKY interaction with FMs stacked in the *z* axis

For the FMs stacked parallel to the z axis (the line connecting two Weyl valleys, see Fig. 1(c), we take $k_\perp = k_z$ and $\mathbf{k}_\parallel = (k_x, k_y)$. Under this consideration, one can use the Eqs. (5)–(7) to simplify the interlayer RKKY interaction $J(R_z)$ as

$$J(R_z) = \sum_{\alpha=x,y,z} J_\alpha(R_z) S_\alpha^T S_\alpha^B + J_{fr}(R_z)\left(S_y^T S_z^B + S_z^T S_y^B\right), \quad (19)$$

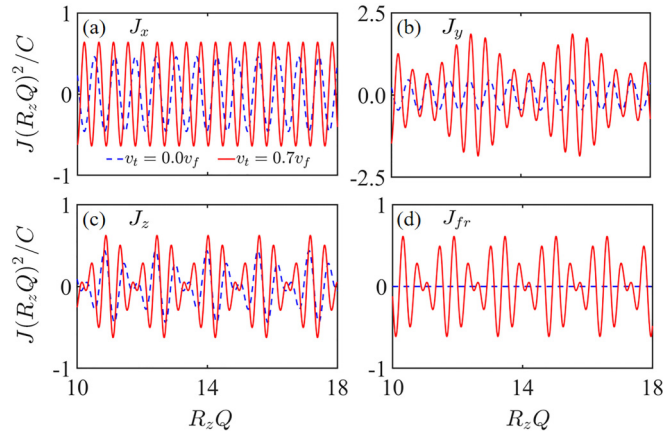

FIG. 6. The spacer thickness R_z-dependent interlayer RKKY components with different tilting parameters. The finite Fermi energy is set as $u_F = 5v_fQ$.

where no DM term emerges but instead a spin-frustrated term appears. The vanished DM term is guaranteed by the protected inversion symmetry of the real-space Green's function, i.e., $G(R_z, ik_n) = G(-R_z, ik_n)$ with $G(\pm R_z, ik_n) = \sum_{k_z,\mathbf{k}_\parallel,\lambda} e^{\pm ik_z R_z} G^\lambda_{k_z,\mathbf{k}_\parallel}(ik_n)$.

For $u_F = 0$, performing some algebraic calculations (see Appendix C), the RKKY components can be solved as

$$\begin{aligned} J_{x,y}(R_z, u_F = 0) &= \sum_{\lambda,\lambda'} \frac{-\pi^3(1 + 3\lambda\lambda')}{6v_f R_z^3} e^{i(\lambda'-\lambda)QR_z}, \\ &= \frac{2\pi^3}{3v_f}\frac{\cos(2QR_z) - 2}{R_z^3}, \\ J_z(R_z, u_F = 0) &= \sum_{\lambda,\lambda'} \frac{\pi^3(\lambda\lambda' - 1)J_c}{6v_f R_z^3} e^{i(\lambda'-\lambda)QR_z}, \\ &= -\frac{2\pi^3 J_c}{3v_f}\frac{\cos(2QR_z)}{R_z^3}, \\ J_{fr}(R_z, u_F = 0) &= 0. \end{aligned} \quad (20)$$

Here, the RKKY components for $u_F = 0$ is also v_t independent due to the elimination of v_t in the energy difference $E_{+,\lambda}(k_z + q_z, k_\parallel) - E_{-,\lambda}(k_z + q_z, k_\parallel)$. Unlike the cases in Secs. III A and III B where there only exists the intravalley contributions, the interlayer RKKY interaction here include both intravalley and intervalley contributions, i.e., $\lambda = \lambda'$ and $\lambda \neq \lambda'$ coexist at the same time. For intervalley case, there emerges an oscillaion factor $\cos(2QR_z)$ or $e^{i(\lambda'-\lambda)QR_z}$, which is induced by the separated projections of Weyl points in the k_z axis, very different from the cases with two FMs stacked in the x and y axis.

For $u_F \neq 0$ and $v_t = 0$, the interlayer RKKY behaviors are significantly different for different components $J_\alpha(R_z)$, as shown by the dashed blue lines in Fig. 6. Specifically speaking, the components $J_{x,y}(R_z)$ exhibit an oscillation with a period $T = \pi v_f/u_F$, stemming from $\sin(2k^0 R_z)$, which is induced by the finite Fermi energy u_F, similar to the cases in previous sections. But, the case for the component $J_z(R_z)$ is different. Beside the u_F-dependent oscillation $\sin(2k^0 R_z)$,

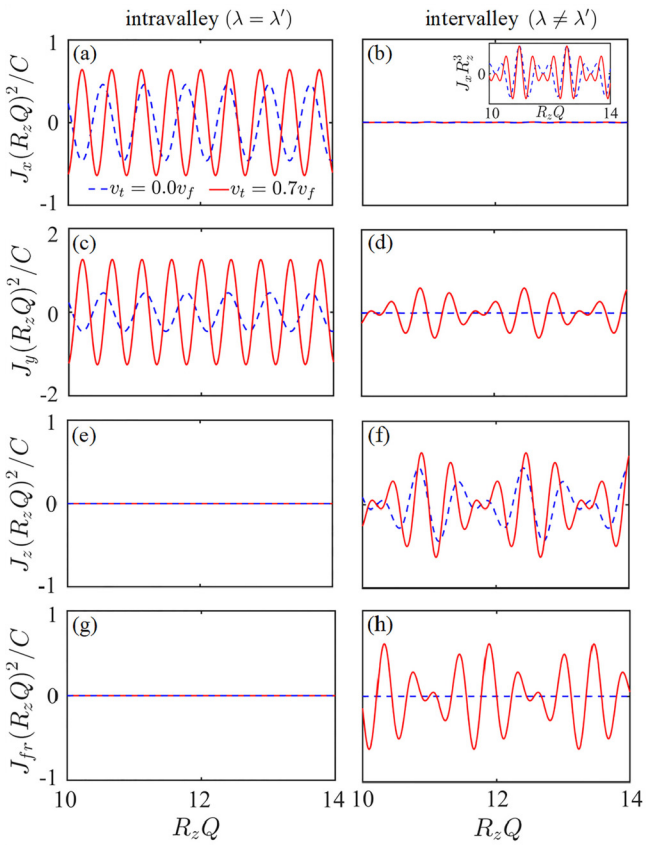

FIG. 7. The intravalley ($\lambda = \lambda'$) and intervalley ($\lambda \neq \lambda'$) terms versus the spacer thickness R_z with different tilting parameters. Other parameters are the same as that in Fig. 6.

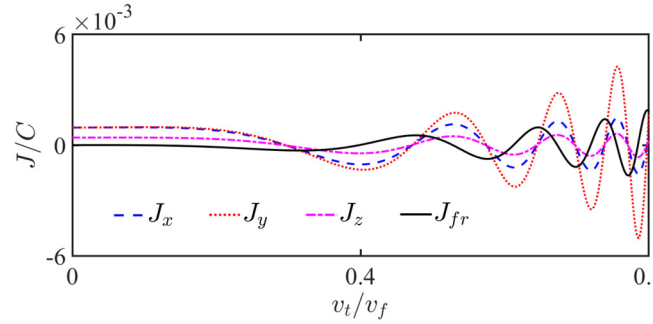

FIG. 8. v_t-dependent interlayer RKKY components with $R_zQ = 12$ and $u_F = 1.5v_fQ$.

$J_z(R_z)$ exhibits another oscillation $\cos(2QR_z)$. The combination of these two oscillations constructs the battering pattern for $J_z(R_z)$, as shown in Fig. 6(c). To understand this phenomenon, it should be noted that both the intravalley ($\lambda = \lambda'$) and intervalley ($\lambda \neq \lambda'$) contributions can support the oscillation $\sin(2k^0R_z)$ as long as $u_F \neq 0$, but the origin of the oscillation $\cos(2QR_z)$ is only related to the intervalley contribution. As shown in Fig. 7 (dashed lines), $J_z(R_z)$ is completely contributed by the intervalley process, so naturally the two-period oscillation survives. Differently, the intervalley part of $J_{x,y}(R_z)$ decays fast as R_z^{-3} and thus the intravalley one with the oscillation $\sin(2k^0R_z)$ decaying as R_z^{-2} dominates in the long range. The results here are different from that in WSMs with magnetic impurities [45,46], where all RKKY components always exhibit a two-period oscillation. The underlying physics is that when the zero-dimensional magnetic impurities are substituted by two-dimensional FMs, the intervalley contributions in $J_{x,y}$ would be suppressed.

For $u_F \neq 0$ and $v_t \neq 0$, there arises two new magnetic signatures for characterizing the tilting effect, which are different from the cases with FMs stacked in x and y axes. One is that the original one-period oscillation of $J_y(R_z)$ is changed to be a battering pattern [Fig. 6(b)]. The reason is that the finite v_t can generate a new intervalley term, whose amplitude is comparable to that of the intravalley term due to the slow-decaying law R_z^{-2}, as shown in Fig. 7(d). The other signature is the nonzero frustrated term $J_{fr}(R_z)$ induced by the finite tilting parameter v_t. Notice that $J_{fr}(R_z)$ is vanished in the absence of v_t even for $u_F \neq 0$, different from the DM interaction as addressed above where only finite u_F is required. This can be understood by checking the expression of $J_{fr}(R_z)$. According to Eqs. (5)–(7), the simplest form of $J_{fr}(R_z)$ can be obtained after some algebraic calculations, given by

$$J_{fr}(R_z) \propto \iint dk_n dk_x \int_{-\infty}^{\infty} dk_y \frac{(\lambda' - \lambda)e^{-2R_zF(k_x,k_y,k_n)}}{F(k_x,k_y,k_n)} k_y, \tag{21}$$

where $F = [k_x^2 + k_y^2 - (ik_n + u_F - v_tk_y)^2/v_f^2]^{1/2}$ and the constant prefactor is dropped for simplicity. Obviously, the integrand in the above equation is an odd function of k_y for $v_t = 0$, leading to $J_{fr} = 0$. Once the tilting effect is turned on ($v_t \neq 0$), the integrand is changed to be neither odd function nor even function, and so nonzero J_{fr} arises. Notice that the spin-frustrated term is unique in FM/WSM/FM systems since this term always vanishes in tilted WSMs doping with magnetic impurities no matter what axis the impurities are placed in [52]. In addition, similar signatures as that in the previous two sections are also found, including the enhancement of the amplitude of the interaction by the increased tilting parameter v_t (Fig. 6), the tilt-modified oscillation $\sin(2k_z^mR_z)$ with $k_z^m = k_x^m$ being the short axis of the projected ellipse in Fig. 2(b), and the magnetism switching by the variation of v_t as shown in Fig. 8.

D. Decaying rate of the interlayer RKKY interaction

From the above results, we know that all the RKKY components always decay with the distance between two FMs as $J(R_\perp) \propto R_\perp^{-3}$ for $u_F = 0$ and $\propto R_\perp^{-2}$ for finite u_F, which exhibit a slower decaying rate compared with the impurity case [45,46] where $J(\mathbf{R}) \propto R^{-5}$ for $u_F = 0$ and $\propto R^{-3}$ for finite u_F. The underlying physics of the difference between them is attributed to the dimensionality effect of the ferromagnetic layers. We find the decaying rate not only depends on the dimension d_h of the spacer but also the one d_F of ferromagnetic layers. In the following discussion, we see that finite d_F not only modifies the amplitude of the interlayer RKKY interaction, but also prolongs its decaying rate.

Before discussing, we first review the RKKY interaction between zero-dimensional magnetic impurities [45,46], which is assumed to be mediated by one Weyl valley for simplicity since the intervalley process does not affect the decaying law.

The results can be solved by the second-order perturbation theory, given by

$$J_\alpha(\mathbf{R}, u_F = 0) \propto \frac{1}{R^{d_h+\zeta}}\left(\frac{5R_\alpha^2}{R^2} - 3\right), \tag{22}$$

where $\alpha = x, y, z$. Here, the decay of the RKKY interaction between magnetic impurities is determined by the dimensionality $d_h = 3$ of WSM host material and the exponent $\zeta = 2$ of its DOS $\rho(\omega) \propto \omega^\zeta$. If the zero-dimensional impurities are substituted by d_F-dimensional ferromagnetic layers, this extra FM's dimensionality d_F is expected to enter into the decaying rate of the RKKY interaction.

To obtain a detailed understanding for the dimensionality effect of deposited FMs, the ferromagnetic layers are assumed to be in-plane infinite, where abundant pointlike magnetic impurities with local spins are continuously and uniformly distributed in. In this view, the interlayer RKKY interaction $J_\alpha(R_\perp)$ evaluates a net RKKY interaction contributed by the total in-plane local spins. Choosing one of the local spins as the origin $\mathbf{S}_0$, the other spins with position $(R_\perp, \mathbf{R}_\parallel)$ would have a specific exchange interaction with $\mathbf{S}_0$. This interaction acts as a $\mathbf{R}_\parallel$-dependent distribution function, which can be approximately represented by $J_\alpha(\mathbf{R}, u_F = 0)$ in Eq. (22). Thus, $J_\alpha(R_\perp)$ can be obtained by considering an integral of $J_\alpha(\mathbf{R}, u_F = 0)$ over $\mathbf{R}_\parallel$, i.e.,

$$J_\alpha(R_\perp, u_F = 0) \propto \int J_\alpha(\mathbf{R}, u_F = 0) d^{d_F}\mathbf{R}_\parallel. \tag{23}$$

$(R_\perp, \mathbf{R}_\parallel)$ is assumed as $R_\perp = R_x$ and $\mathbf{R}_\parallel = (R_y, R_z)$ for simplicity. In this way, the dimensionality d_F is introduced to connect the RKKY interaction $J_\alpha(\mathbf{R}, u_F = 0)$ of local spins with the interlayer RKKY interaction $J_\alpha(R_\perp, u_F = 0)$. Using Eqs. (22) and (23), we find that the net in-plane interaction $J_\alpha(R_\perp, u_F = 0)$ has the following decaying rate,

$$J_{y,z}(R_\perp, u_F = 0) \propto \frac{1}{R_\perp^{d_h+\zeta-d_F}}, \tag{24}$$

and $J_x = 0$. The obtained Eq. (24) has generality. In our study, the layered FMs deposited in WSMs is two dimension $d_F = 2$, so $J_{y,z} \propto 1/R_\perp^{d_h+\zeta-d_F} = 1/R_\perp^{3+2-2} = 1/R_\perp^3$ recovers the results in Eq. (14). Taking $d_F = 0$, corresponding to zero-dimensional pointlike magnetic impurities, the decaying rate of RKKY interaction recalls the recent results in WSMs [45,46]. Recently, the RKKY interaction between one-dimensional ferromagnetic chains, which is mediated by two-dimensional topological surface states ($d_h = 2$, $\zeta = 1$), has been reported and falls off as [51] $1/R_\perp^2$ ($u_F = 0$). This interaction still follows the law of Eq. (24) by setting $d_F = 1$. Compared with Eq. (22), the dimension d_F of FM layers in Eq. (24) take an important role to prolong the decaying rate, as stated in our results.

For $u_F \neq 0$, following the same calculation process as above, the general law for the interlayer RKKY interaction can be obtained as

$$J_\alpha(R_\perp, u_F \neq 0) \propto \frac{u_F^{d_h-1-d_F/2}}{R_\perp^{d_h-d_F/2}} \sin(2k_0 R_\perp + \eta), \tag{25}$$

where η is a fitted constant. This law explains the numerical results in Fig. 3. Compared to the law of $u_F = 0$ in Eq. (24), the introduction of finite Fermi energy eliminates the decaying term $R^{\zeta-d_F/2}$, which further prolongs the decay of interlayer interaction. For $d_F = 0$, the result in Eq. (25) is reminiscence of the RKKY interaction ($u_F \neq 0$) between magnetic impurities in WSMs [45,46].

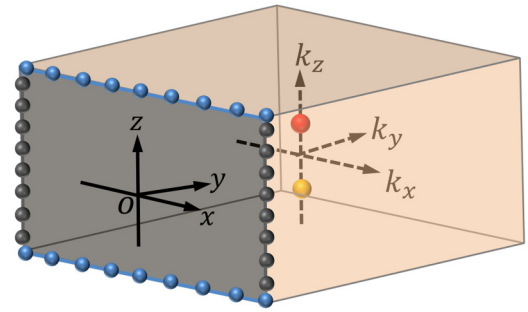

FIG. 9. Schematic diagram for a semi-infinite WSM, which is infinite along the x (or z) axis and is terminated in the y axis with its surface at $y = 0$. The black (blue) edges of ferromagnetic layers are parallel (perpendicular) to the line connected Weyl nodes.

E. Interlayer RKKY interaction mediated by Fermi arc

In above discussions, the WSM is assumed to be infinite. In practice, the sample should be finite and Fermi arcs would arise on the surface of WSMs, which will play a role on the RKKY interaction. We find that the Fermi arcs lying on top or bottom layer have negligible contribution. This is because the RKKY interaction is an indirect magnetic interaction, which is mediated by the itinerant electrons between two ferromagnetic layers. In this section, we focus on the effect of Fermi arcs lying between top and bottom ferromagnetic layers.

We consider a semi-infinite WSM, as shown in Fig. 9 where a WSM is placed in the right half-plane ($y > 0$) and the other half ($y < 0$) is assumed to be a vacuum, and is infinite in other two (x and z) directions. Surface states would appear on the $x - z$ plane due to the nontrivial topological properties of WSMs. Since the surface mainly affects the RKKY interaction between the edges of top and bottom ferromagnetic layers, we only need to consider how the Fermi arcs contribute to the RKKY interaction between two ferromagnetic chains, as shown in Fig. 9.

In order to calculate the surface state in the semi-infinite WSM, one has to employ a WSM model with higher-order momentums, which is generally described with [60]

$$H = \xi\left(k_z^2 - Q^2\right)\sigma_z + v_f(k_x\sigma_x + k_y\sigma_y) + C_0 k_x^2, \tag{26}$$

where the term $C_0 k_x^2$ breaks the electron-hole symmetry and would bend the surface band to generate a Fermi arc connecting two Weyl nodes located at $(0, 0, \pm Q)$. Expanding the above Hamiltonian around the Weyl points and retaining the linear terms, one can obtain the same linearized model as that in Eq. (1). Here, we drop the tilting term $v_t k_y$ and only focus on the effect of the Fermi arc on the interlayer exchange interaction. An incident wave $Ce^{-ik_y y}$ is assumed to be injected along $-y$ direction. Near the interface, if the wave is bound to the $x - z$ surface, the solution of the operator k_y becomes imaginary. By considering the continuity conditions of the boundary between $y < 0$ and $y > 0$ regions, the surface band

can be derived as

$$E_{\rm sur} = v_f k_x + C_0 k_x^2, \tag{27}$$

in the range of $-Q < k_z < Q$ and vanishes otherwise. The corresponding wave function of the surface state reads

$$\Psi_{\rm sur} = \sqrt{\frac{\xi\left(Q^2 - k_z^2\right)}{v_f}}\begin{pmatrix}1\\1\end{pmatrix}. \tag{28}$$

By using Eq. (5), one can obtain the formula for the RKKY interaction between two magnetic chains [51], which is mediated by the 2D surface band and given by

$$J(R_\perp) = -\sum_{\alpha,\beta=x,y,z}\frac{S_\alpha^T S_\beta^B J_0^2 a^2}{4\pi A_0^2}\int_{-\infty}^{\infty} dq_\perp e^{iq_\perp R_\perp}\chi_{\alpha\beta}(q_\perp), \tag{29}$$

where A_0 is the area of the unit cell projected on the $x-z$ plane, $S_\alpha^T(S_\beta^B)$ is the spin of the top (bottom) magnetic chain. The static spin susceptibility tensor $\chi_{\alpha\beta}(q_\perp)$ reads as

$$\chi_{\alpha\beta}(q_\perp) = -\frac{\mu_B^2}{\gamma}\sum_{ik_n,\mathbf{k}}{\rm Tr}[G_{k_\perp,k_\parallel}(ik_n)\sigma_\alpha G_{k_\perp+q_\perp,k_\parallel}(ik_n)\sigma_\beta], \tag{30}$$

where $\mathbf{k} = (k_\perp, k_\parallel)$ and the subscript $\perp$ ($\parallel$) represents the direction perpendicular (parallel) to magnetic chains. Using the eigenvalues and eigenfunctions in Eqs. (27)–(28), the Matsubara Green's function $G_{k_\perp,k_\parallel}(ik_n)$ can be constructed as

$$G_{k_\perp,k_\parallel}(ik_n) = \frac{\Psi_{\rm sur}\Psi_{\rm sur}^+}{ik_n - E_{\rm sur}} = \frac{\xi\left(Q^2 - k_z^2\right)\Theta\left(Q^2 - k_z^2\right)\rho_0/v_f}{ik_n + u_F - v_f k_x - C_0 k_x^2}, \tag{31}$$

where $\rho_0 = \sigma_0 + \sigma_x$ (σ_0 is the identity matrix). Due to Fermi arc arising along the separated Weyl points, there will appear two types of arrangements of the magnetic chains, namely, the magnetic chains are parallel to the line connected Weyl nodes, corresponding to Figs. 1(a) and 1(b), and perpendicular to the line as in Fig. 1(c).

For the case with two magnetic chains parallel to the line connected Weyl nodes, as indicated by black color in Fig. 9, we take $(k_\perp, k_\parallel) = (k_x, k_z)$. Substituting Eqs. (30)–(31) into Eq. (29), the formula for the exchange RKKY interaction mediated by the Fermi arc can be rewritten as

$$J(R_x) = \sum_{\alpha,\beta=x,y,z} S_\alpha^T S_\beta^B J_c' \int_{-\infty}^{\infty} dq_x' \int_{-\infty}^{\infty} dk_n \int_{-\infty}^{\infty} dk_x \int_{-Q}^{Q} dk_z \frac{e^{i(q_x'-k_x)R_x}\left(Q^2 - k_z^2\right)^2 {\rm Tr}(\rho_0\sigma_\alpha\rho_0\sigma_\beta)}{32\left(ik_n + u_F - v_f k_x - C_0 k_x^2\right)\left(ik_n + u_F - v_f q_x' - C_0 q_x'^2\right)}, \tag{32}$$

where $J_c' = J_0^2 a^2 \mu_B^2 \xi^2/(\pi^4 v_f^2 A_0^2)$ and the coordinate transformation $k_x + q_x = q_x'$ is used.

Summing over the indices for spin, one can find that only the RKKY component $J_x(R_x)S_x^T S_x^B$ survives, which is the out-of-plane component and is lacking for bulk states as discussed in Secs. III A and III B in the absence of tilt. After some algebraic calculations, $J_x(R_x)$ can be simplified as

$$J_x(R_x) = \int_{-\infty}^{\infty} dk_n \frac{-16\pi^2 Q^5 J_c' e^{-R_x\sqrt{-4C_0(ik_n+u_F)-v_f^2}/C_0}}{15\left[4C_0(ik_n+u_F)+v_f^2\right]}. \tag{33}$$

According to the above equation, we plot the numerical results of $J_x(R_x)$ in Fig. 10. The exchange RKKY interaction $J_x(R_x)$ falls off slowly as $1/R_x$, along with an oscillation $\cos(2k_0' R_x)$. Compared to the bulk contributions $J_{y(z)}(R_x)$ shown in Fig. 3, there are two main differences: (i) The interaction here decays much more slowly than the bulk contributions ($1/R_x^3$ or $1/R_x^2$), which is ascribed to the anisotropic surface band, i.e., nearly linear dispersion in k_x axis and dispersionless in k_z axis. It is worth noting that the surface contribution in WSM decays much slowly than the interlayer RKKY interaction mediated by the helical surface states of topological insulator ($1/R^{3/2}$ for $u_F \neq 0$) [51]. This suggests that WSMs are more promising materials with application potential to manipulate spins of magnetic chains. (ii) The amplitude of the RKKY component J_x decreases with the increased Fermi energy u_F, but does not change the decay rate of R_x^{-1}. The case here is in contrast to bulk contributions, where $J \propto u_F$ in Fig. 3(b). To understand this phenomenon, one can check the DOS of the surface band $\rho(\omega) = \rho_0/\sqrt{v_f^2 + 4C_0\omega}$, where $\rho_0 = 4\xi Q^3/(3v_f\pi^2)$. Noting that $\rho(\omega)$ decreases with ω, so the number of electrons participated in the magnetic scattering is decreased as u_F increases, and then the amplitude of the interlayer RKKY interaction J_x is decreased.

For the case with two magnetic chains perpendicular to the line connected Weyl nodes, as indicated by blue color in Fig. 9, i.e., $(k_\perp, k_\parallel) = (k_z, k_x)$, utilizing Eqs. (29)–(31) and processing the similar calculations, one can obtain the ana-

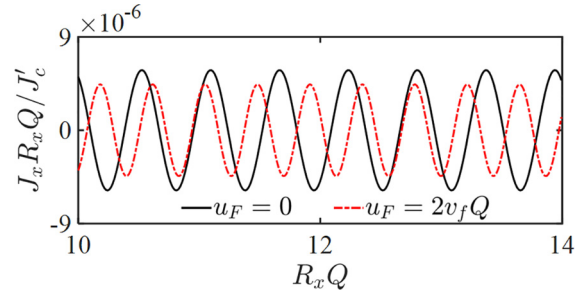

FIG. 10. Dependence of the interlayer RKKY component J_x on the spacer thickness R_x for different Fermi energies u_F. The period of the oscillation is π/k_0' with $k_0' = \sqrt{v_f^2 + 4C_0 u_F}/(2C_0)$. Other parameters are set as: $C_0 = 1$ and $J_c' = J_0^2 a^2 \mu_B^2 \xi^2/(\pi^4 v_f^2 A_0^2)$.

lytical result for the $J_x(R_z)$

$$J_x(R_z) = -\frac{8\pi J_c'[-QR_z\cos(QR_z)+\sin(QR_z)]^2}{\sqrt{4C_0u_F+v_f^2R_z^6}}. \quad (34)$$

Compared with the slowly decaying interaction $J_x(R_x) \propto 1/R_x$, the interaction here falls off fast as $J_x(R_z) \propto 1/R_z^4$. The underlying physics is attributed to the weak dispersion band along k_z axis, where the scattering of electrons between magnetic chains is limited by the zero Fermi velocity $v_z = 0$. In this case, the bulk contribution to J would play a leading role even near the surface since $J \propto 1/R_z^2$ for $u_F \neq 0$ ($J \propto 1/R_z^3$ for $u_F = 0$), and so the effect of the Fermi arcs can be ignored.

IV. CONCLUSION

We have investigated the interlayer RKKY interaction in FM/WSM/FM trilayer system in the presence of the tilting effect of Weyl cones. Our investigation focuses on the influence of the unique features of WSMs: anisotropy dispersion, tilt effect, intervalley transitions, and Fermi arc states. We notice that recently, the interlayer RKKY interaction has been studied with TI film [49,50] or the bulk Rashba semiconductors [51] as the spacer. In Ref. [49], authors show that the TI states contributing to the proximity effect can be directly identified through the change of RKKY coupling with the external magnetic field or Fermi level. In Ref. [50], they focused on the thickness dependence of TI film and found that the RKKY amplitude is not monotonically dependent on the thickness due to the hybridization between surfaces of the TI film. Both of these works did not discuss the RKKY properties that we care about, such as spin models, oscillation period, and decaying rate.

In Ref. [51], authors investigated the interlayer RKKY coupling mediated by a bulk Rashba semiconductor, consisting of intraband and interband contributions and discussed the long-range dependence of different RKKY components (controlled by the FM's relative direction), including the oscillation period and spatial long-range decaying rate in trivial and topological phases. In our paper, we use WSM as spacer and also discuss spin models and long-range decaying rate caused by the unique features of WSM: anisotropy dispersion, tilt effect, and intervalley transitions. In spite of different physics origin, it is interesting to compare our results with Ref. [51]:

(i) Due to the separation of Weyl nodes, the RKKY behaviors, such as spin model, decaying rate, and oscillation period, heavily depend on the stacked direction of FMs. In the topological materials with a single Dirac cone [51], the RKKY interaction is independent of the stacked direction of FMs due to isotropy.

(ii) Noncollinear terms (DM or spin-frustrated terms) always emerge even for the contribution of bulk band. But noncollinear terms vanish for bulk band and appear only for surface states in Ref. [51]. Also, notice that the spin-frustrated term is unique in our system since this term vanishes in Ref. [51] and in tilted WSMs doping with magnetic impurities [45,46].

(iii) We find the tilt has significant effect: (a) Tilt can increase the RKKY magnitude and change XYY to XYZ spin model. (b) Tilt can make RKKY interaction switch between antiferromagnetism and ferromagnetism. (c) Tilt can lead to spin-frustrated term and change one-period oscillation to battering pattern. Furthermore, we obtain a simply analytical expression Eq. (16) about oscillation period, from which one can easily extract the tilt parameter. But no tilt is presented in Ref. [51].

(iv) Intervalley transition due to separated Weyl nodes generates extra oscillation with period determined by separated distance Q between Weyl nodes. This new oscillation together with Fermi-energy-induced oscillation leads to an interesting battering pattern. Notice that it is essentially different from the intraband and interband transitions stemming from the splitting of Rashba spin-orbit interaction in Ref. [51]. Although the intraband and interband transitions can cause different periods of oscillation, the total oscillation is their summation, which cannot lead to battering pattern.

(v) Anisotropic surface states can lead to much slower RKKY decaying rate (R^{-1}) than those mediated by the helical surface states of TIs ($R^{-3/2}$) in Ref. [51]. Notice, in WSMs, both bulk and surface states contribute to the RKKY interaction, but only the contribution either from bulk or surface states exists in Ref. [51].

In addition, we find the decaying rate not only depends on the dimension of the spacer but also the one of ferromagnetism, and obtained Eq. (24) has generality, which recalls previous results. Thus, we explain the origin of slower-decaying rate of interlayer RKKY interaction, compared with the impurity case. Therefore, we exhibit significant unique RKKY characteristics of WSMs, which are helpful to understand the WSM magnetic property and to extract the parameters of WSM materials.

In summary, we have investigated the interlayer RKKY interaction in FM/WSM/FM trilayer system. Different arrangements of the ferromagnetic layers are considered to discuss the magnetic anisotropy. By comparing the cases of tilted with untilted WSMs, rich signatures are extracted from the interlayer interaction to characterize the tilting effect, including anisotropic XYZ spin models, magnetization switchings, modified oscillatory patterns, and newly emerged spin-frustrated terms. Due to the dimensionality effect of the ferromagnetic layers, the latter two signatures are significantly different with that from the RKKY interaction of magnetic impurities as reported in previous literatures. In addition, this effect can result in a slower-decaying law for the interlayer RKKY interaction, which makes the magnetic signatures easier to be detected. We further discuss the effect of surface states on the interlayer RKKY interaction at the edges of ferromagnetic layer. When the ferromagnetic layer edges are parallel to the line connecting the Weyl nodes, we find a more slowly decaying law, compared with bulk contribution. On the whole, our work suggests that trilayer systems are more powerful platforms for characterizing the intrinsic properties of topological materials. All interlayer RKKY signatures are expected to be probed experimentally with present techniques, e.g., the broadband ferromagnetic resonance [54], which can detect the acoustic and optic modes to evaluate the different effective magnetizations of the two ferromagnetic layers, or

the magneto-optic Kerr effect [55,61] to investigate the hysteresis loop.

ACKNOWLEDGMENTS

This work was supported, by the National Natural Science Foundation of China (Grants No. 12104167, No. 12174121, and No. 11904107), by the Science and Technology Program of Guangzhou (No. 2019050001), by the Guangdong NSF of China (Grants No. 2021A1515011566 No. 2021A1515010369, and No. 2021A1515010369).

Y.-J.W. and Q.-Y.X. contributed equally to this work.

APPENDIX A: INTERLAYER RKKY INTERACTION WITH FMS STACKED IN THE *x* AXIS

In this section, we consider the arrangement of FMs with their stacking direction parallel to the x axis, i.e., $k_\perp = k_x$ and $\mathbf{k}_\parallel = (k_y, k_z)$. Utilizing Eqs. (2), (3), and (7) of the main text, one can obtain the Matsubara Green's function of $u_F = 0$ as

$$G^{\lambda}_{k_x+q_x,\mathbf{k}_\parallel}(ik_n) = \frac{ik_n - v_t k_y + H_0(k_x+q_x,\mathbf{k}_\parallel)}{(ik_n - v_t k_y)^2 - \varepsilon^2(k_x+q_x,\mathbf{k}_\parallel)}, \tag{A1}$$

with

$$\begin{aligned} H_0(k_x,\mathbf{k}_\parallel) &= v_f[k_x\sigma_x + k_y\sigma_y + \lambda(k_z - \lambda Q)\sigma_z], \\ \varepsilon(k_x,\mathbf{k}_\parallel) &= \pm v_f\sqrt{k_x^2 + k_y^2 + (k_z - \lambda Q)^2}. \end{aligned} \tag{A2}$$

where $H_0(k_x,\mathbf{k}_\parallel)$ is the Hamiltonian of nontilted WSMs with the corresponding energy $\varepsilon(k_x,\mathbf{k}_\parallel)$. By simply setting $q_x = 0$ in Eq. (A1), $G^{\lambda}_{k_x,\mathbf{k}_\parallel}(ik_n)$ can be obtained. Since the projections of two Weyl valleys in the k_x axis are completely overlapped, they would contribute equally to the interlayer RKKY interaction, i.e., $\lambda' = \lambda$ in the Eq. (6) of the main text. Substituting the Eq. (A1) to the Eq. (6) of the main text, the static spin susceptibility $\chi_{\alpha\beta}(0,q_x)$ can be simplified as

$$\begin{aligned} \chi_{\alpha\beta}(0,q_x) &= \frac{-\mu_B^2}{\gamma}\sum_{\lambda,k_n,\mathbf{k}} \frac{\mathrm{Tr}\{[ik_n - v_t k_y + H_0(k_x,\mathbf{k}_\parallel)]\sigma_\alpha[ik_n - v_t k_y + H_0(k_x+q_x,\mathbf{k}_\parallel)]\sigma_\beta\}}{[(k_n + iv_t k_y)^2 + \varepsilon^2(k_x,\mathbf{k}_\parallel)][(k_n + iv_t k_y)^2 + \varepsilon^2(k_x+q_x,\mathbf{k}_\parallel)]}, \\ &= \frac{-\mu_B^2}{(2\pi)^4}\sum_{\lambda}\int dk_n \int d\mathbf{k} \frac{\mathrm{Tr}\{[ik_n - v_t k_y + H_0(k_x,\mathbf{k}_\parallel)]\sigma_\alpha[ik_n - v_t k_y + H_0(k_x+q_x,\mathbf{k}_\parallel)]\sigma_\beta\}}{[(k_n + iv_t k_y)^2 + \varepsilon^2(k_x,\mathbf{k}_\parallel)][(k_n + iv_t k_y)^2 + \varepsilon^2(k_x+q_x,\mathbf{k}_\parallel)]}, \end{aligned} \tag{A3}$$

where $\mathbf{k} = (k_x,\mathbf{k}_\parallel)$ with $\mathbf{k}_\parallel = (k_y,k_z)$.

To avoid the divergent integrals in the Eq. (A3), one can use the following Feynman parametrization [59]:

$$\begin{aligned} &\frac{1}{(k_n + iv_t k_y)^2 + \varepsilon^2(k_x,\mathbf{k}_\parallel)}\frac{1}{(k_n + iv_t k_y)^2 + \varepsilon^2(k_x+q_x,\mathbf{k}_\parallel)} \\ &= \int_0^1 dg \frac{1}{\{g[(k_n + iv_t k_y)^2 + \varepsilon^2(k_x+q_x,\mathbf{k}_\parallel)] + (1-g)[(k_n + iv_t k_y)^2 + \varepsilon^2(k_x,\mathbf{k}_\parallel)]\}^2} \\ &= \int_0^1 dg \frac{1}{\left[(k_n + iv_t k_y)^2 + \varepsilon^2(k_x,\mathbf{k}_\parallel) + gq_x v_f^2(2k_x + q_x)\right]^2}. \end{aligned} \tag{A4}$$

In this way, the static spin susceptibility $\chi_{\alpha\beta}(0,q_x)$ can be expressed as

$$\chi_{\alpha\beta}(0,q_x) = \frac{-\mu_B^2}{(2\pi)^4}\sum_{\lambda}\iint dk_n d\mathbf{k}\int_0^1 dg \frac{\mathrm{Tr}\{[ik_n - v_t k_y + H_0(k_x,\mathbf{k}_\parallel)]\sigma_\alpha[ik_n - v_t k_y + H_0(k_x+q_x,\mathbf{k}_\parallel)]\sigma_\beta\}}{\left[(k_n + iv_t k_y)^2 + \varepsilon^2(k_x,\mathbf{k}_\parallel) + gq_x v_f^2(2k_x + q_x)\right]^2}. \tag{A5}$$

Using the coordinate transformation $(k_x + gq_x, k_z - \lambda Q) = (k_x', k_z')$, the above equation can be further simplified as

$$\chi_{\alpha\beta}(0,q_x) = \frac{-\mu_B^2}{(2\pi)^4}\sum_{\lambda}\iint dk_n d\mathbf{k}'\int_0^1 dg \frac{\mathrm{Tr}\{[ik_n - v_f gq_x\sigma_x + h(\mathbf{k}')]\sigma_\alpha[ik_n + v_f q_x(1-g)\sigma_x + h(\mathbf{k}')]\sigma_\beta\}}{\left[(k_n + iv_t k_y)^2 + v_f^2|\mathbf{k}'|^2 + g(1-g)v_f^2 q_x^2\right]^2}, \tag{A6}$$

with

$$h(\mathbf{k}') = -v_t k_y + v_f(k_x'\sigma_x + k_y\sigma_y + \lambda k_z'\sigma_z), \tag{A7}$$

where $\mathbf{k}' = (k_x',\mathbf{k}_\parallel')$ with $\mathbf{k}_\parallel' = (k_y,k_z')$. Plugging $\chi_{\alpha\beta}(0,q_x)$ into the Eq. (5) of the main text and tracing over the Pauli matrices, the interlayer RKKY interaction $J(R_x)$ can be split into the following terms:

$$J(R_x) = \sum_{\alpha=x,y,z} J_\alpha(R_x) S_\alpha^T S_\alpha^B + J_x^{DM}(R_x)(\mathbf{S}^T \times \mathbf{S}^B)_x, \tag{A8}$$

with

$$\frac{J_x(R_x)}{J_c}=\int_{-\infty}^{\infty}dq_x e^{iq_xR_x}\int_{-\infty}^{\infty}d\mathbf{k}'\int_{-\infty}^{\infty}dk_n\int_0^1 dg\quad\frac{(ik_n-v_tk_y)^2+v_f^2\left[(k_x'-gq_x)(k_x'+q_x-gq_x)-k_y^2-k_z{}^2\right]}{\left[(k_n+iv_tk_y)^2+v_f^2|\mathbf{k}'|^2+g(1-g)v_f^2q_x^2)\right]^2},$$

$$\frac{J_y(R_x)}{J_c}=\int_{-\infty}^{\infty}dq_x e^{iq_xR_x}\int_{-\infty}^{\infty}d\mathbf{k}'\int_{-\infty}^{\infty}dk_n\int_0^1 dg\frac{(ik_n-v_tk_y)^2+v_f^2\left[k_y^2-k_z'^2-(k_x'-gq_x)(k_x'+q_x-gq_x)\right]}{\left[(k_n+iv_tk_y)^2+v_f^2|\mathbf{k}'|^2+g(1-g)v_f^2q_x^2)\right]^2},$$

$$\frac{J_z(R_x)}{J_c}=\int_{-\infty}^{\infty}dq_x e^{iq_xR_x}\int_{-\infty}^{\infty}d\mathbf{k}'\int_{-\infty}^{\infty}dk_n\int_0^1 dg\frac{(ik_n-v_tk_y)^2+v_f^2\left[k_z'^2-k_y^2-(k_x'-gq_x)(k_x'+q_x-gq_x)\right]}{\left[(k_n+iv_tk_y)^2+v_f^2|\mathbf{k}'|^2+g(1-g)v_f^2q_x^2)\right]^2},$$

$$\frac{J_x^{DM}(R_x)}{J_c}=\int_{-\infty}^{\infty}dq_x e^{iq_xR_x}\int_{-\infty}^{\infty}d\mathbf{k}'\int_{-\infty}^{\infty}dk_n\int_0^1 dg\frac{-iv_fq_x(ik_n-v_tk_y)}{\left[(k_n+iv_tk_y)^2+v_f^2|\mathbf{k}'|^2+g(1-g)v_f^2q_x^2)\right]^2},\tag{A9}$$

where $J_c=J_0^2\mu_B^2a^2/(16\pi^5V_0^2)$, $J_\alpha(R_x)$ couples collinear spins and $J_x^{DM}(R_x)$ describes the DM (noncollinear) interaction.

We take $J_y(R_x)$ as an example to show the detail calculation process, which is given by

$$\begin{aligned}
J_y(R_x)&=\int_{-\infty}^{\infty}dq_x e^{iq_xR_x}\int_{-\infty}^{\infty}d\mathbf{k}'\int_{-\infty}^{\infty}dk_n\int_0^1 dg\frac{(ik_n-v_tk_y)^2+v_f^2\left[k_y^2-k_z'^2-(k_x'-gq_x)(k_x'+q_x-gq_x)\right]}{\left[(k_n+iv_tk_y)^2+v_f^2|\mathbf{k}'|^2+g(1-g)v_f^2q_x^2\right]^2J_c^{-1}}\\
&=\int dq_x e^{iq_xR_x}\int dk_x'\int dk_y\int dk_n\int_0^1 dg\frac{\pi J_c\left[(ik_n-v_tk_y)^2-v_f^2k_x'^2\right]}{v_f\left[(k_n+iv_tk_y)^2+v_f^2k_x'^2+v_f^2k_y^2+g(1-g)v_f^2q_x^2\right]^{\frac{3}{2}}}\\
&=\int dk_x'\int dk_y\int dk_n\int_{-\infty}^{\infty}dq_x e^{iq_xR_x}\frac{\left[(k_n+iv_tk_y)^2+v_f^2k_x'^2+v_f^2k_y^2\right]^{-\frac{1}{2}}\left[(ik_n-v_tk_y)^2-v_f^2k_x'^2\right]}{v_f\left[4(k_n+iv_tk_y)^2+4v_f^2k_x'^2+4v_f^2k_y^2+v_f^2q_x^2\right](4\pi J_c)^{-1}}\\
&=\int_{-\infty}^{\infty}dk_x'\int_{-\infty}^{\infty}dk_y\int_{-\infty}^{\infty}dk_n\frac{e^{-\frac{2R_x\sqrt{\left(k_n+i\frac{v_t}{v_f}k_y\right)^2+k_x'^2+k_y^2}}{v_f}}2\pi^2\left[\left(ik_n-\frac{v_t}{v_f}k_y\right)^2-k_x'^2\right]}{v_f^4\left[\left(k_n+i\frac{v_t}{v_f}k_y\right)^2+k_x'^2+k_y^2\right]J_c^{-1}}\\
&=\int_0^{\pi}\sin(\theta)d\theta\int_0^{2\pi}d\varphi\int_0^{\infty}k^2dk\frac{\left(2\pi^2J_c/v_f^4\right)\left\{\left[i\cos(\theta)-\frac{v_t\sin(\theta)\sin(\varphi)}{v_f}\right]^2-[\sin(\theta)\cos(\varphi)]^2\right\}}{e^{\frac{2R_xk\sqrt{\left[\cos(\theta)+\frac{iv_t\sin(\theta)\sin(\varphi)}{v_f}\right]^2+\sin^2(\theta)}}{v_f}}\left\{\left[\cos(\theta)+\frac{iv_t\sin(\theta)\sin(\varphi)}{v_f}\right]^2+\sin^2(\theta)\right\}}\\
&=\int_0^{\pi}d\theta\int_0^{2\pi}d\varphi\frac{-\pi^2\sin(\theta)\left\{\cos^2(\varphi)\sin^2(\theta)+\left[\cos(\theta)+\frac{iv_t\sin(\theta)\sin(\varphi)}{v_f}\right]^2\right\}J_c}{2v_fR_x^3\left\{\sin^2(\theta)+\left[\cos(\theta)+\frac{iv_t\sin(\theta)\sin(\varphi)}{v_f}\right]^2\right\}^{\frac{5}{2}}}\\
&=\int_0^{2\pi}d\varphi\frac{-\pi^2[2+\cos(2\varphi)]J_c}{3v_fR_x^3}=-\frac{4\pi^3J_c}{3v_f}\frac{1}{R_x^3}.
\end{aligned}\tag{A10}$$

As shown above, the tilting effect does not affect the interlayer RKKY interaction of zero Fermi energy $u_F=0$. The reason is that the interlayer interaction of $u_F=0$ is only determined by the energy difference [51] $E_{+,\lambda}(k_x,k_\parallel)-E_{-,\lambda}(k_x+q_x,k_\parallel)$ [Eq. (2) of the main text], which is independent on the parameter v_t and naturally leads to unperturbed results even in the presence of the tilting effect.

Following the similar integration process, one can obtain $J_z(R_x)=J_y(R_x)$, $J_x(R_x)=0$ and $J_x^{DM}(R_x)=0$. Obviously, the collinear interlayer RKKY components exhibit a XYY spin model, i.e., $J_x(R_x)\neq J_y(R_x)=J_z(R_x)$. Noting that the vanished out-of-plane collinear component $J_x(R_x)$ is induced by the dimensional effect of ferromagnetic layers, as discussed in the main text.

APPENDIX B: INTERLAYER RKKY INTERACTION WITH FMS STACKED IN *y* AXIS

For the arrangement of FMs with their stacking direction parallel to the y axis, i.e., $k_\perp=k_y$ and $\mathbf{k}_\parallel=(k_z,k_x)$. Utilizing Eqs. (2), (3), and (7) of the main text, the Matsubara Green's function $G^{\lambda}_{k_y,\mathbf{k}_\parallel}(ik_n)$ of $u_F=0$ can be constructed as

$$G^{\lambda}_{k_y+q_y,\mathbf{k}_\parallel}(ik_n)=\frac{ik_n-v_t(k_y+q_y)+H_0(k_y+q_y,\mathbf{k}_\parallel)}{[ik_n-v_t(k_y+q_y)]^2-\varepsilon^2(k_y+q_y,\mathbf{k}_\parallel)}.\tag{B1}$$

Similar to the case with ferromagnetic layers stacked in the x axis, the interlayer RKKY interaction here is only contributed by the intravalley coupling, i.e., $\lambda=\lambda'$ still holds in

the Eq. (6) of the main text. Following the similar process in the Appendix A, one can use the Eq. (B1) and Eqs. (5)–(6) of the main text to simplify the interlayer RKKY interaction $J(R_y)$ as

$$J(R_y) = \sum_{\alpha=x,y,z} J_\alpha(R_y) S_\alpha^T S_\alpha^B + J_y^{DM}(R_y)(\mathbf{S}^T \times \mathbf{S}^B)_y, \tag{B2}$$

with

$$\frac{J_x(R_y)}{J_c} = \int_{-\infty}^{\infty} dq_y e^{iq_y R_y} \int_{-\infty}^{\infty} d\mathbf{k}' \int_{-\infty}^{\infty} dk_n \int_0^1 dg \frac{f(g)f(g-1) + v_f^2 k_x^2 - v_f^2(k_y' - gq_y)(k_y' - gq_y + q_y) - v_f^2 k_z'^2}{\left[(k_n + iv_t k_y')^2 + v_f^2|\mathbf{k}'|^2 + \left(v_f^2 - v_t^2\right)g(1-g)q_y^2\right]^2},$$

$$\frac{J_y(R_y)}{J_c} = \int_{-\infty}^{\infty} dq_y e^{iq_y R_y} \int_{-\infty}^{\infty} d\mathbf{k}' \int_{-\infty}^{\infty} dk_n \int_0^1 dg \frac{f(g)f(g-1) - v_f^2 k_x^2 + v_f^2(k_y' - gq_y)(k_y' - gq_y + q_y) - v_f^2 k_z'^2}{\left[(k_n + iv_t k_y')^2 + v_f^2|\mathbf{k}'|^2 + \left(v_f^2 - v_t^2\right)g(1-g)q_y^2\right]^2},$$

$$\frac{J_z(R_y)}{J_c} = \int_{-\infty}^{\infty} dq_y e^{iq_y R_y} \int_{-\infty}^{\infty} d\mathbf{k}' \int_{-\infty}^{\infty} dk_n \int_0^1 dg \frac{f(g)f(g-1) - v_f^2 k_x^2 - v_f^2(k_y' - gq_y)(k_y' - gq_y + q_y) + v_f^2 k_z'^2}{\left[(k_n + iv_t k_y')^2 + v_f^2|\mathbf{k}'|^2 + \left(v_f^2 - v_t^2\right)g(1-g)q_y^2\right]^2},$$

$$\frac{J_y^{DM}(R_y)}{J_c} = \int_{-\infty}^{\infty} dq_y e^{iq_y R_y} \int_{-\infty}^{\infty} d\mathbf{k}' \int_{-\infty}^{\infty} dk_n \int_0^1 dg \frac{-v_f q_y k_n}{\left[(k_n + iv_t k_y')^2 + v_f^2|\mathbf{k}'|^2 + \left(v_f^2 - v_t^2\right)g(1-g)q_y^2\right]^2},$$

where $f(g) = ik_n - v_t k_y' + g v_t q_y$, $\mathbf{k}' = (k_x, k_y', k_z')$, the Feynman parameterization is similar to the Eq. (A4) and the coordinate transformation $(k_y + gq_y, k_z - \lambda Q) = (k_y', k_z')$ are used.

Taking $J_x(R_y)$ as an example, the integration can be solved as

$$\begin{aligned}
J_x(R_y) &= J_c \int_{-\infty}^{\infty} dq_y e^{iq_y R_y} \int_{-\infty}^{\infty} d\mathbf{k}' \int_{-\infty}^{\infty} dk_n \int_0^1 dg \frac{f(g)f(g-1) + v_f^2 k_x^2 - v_f^2(k_y' - gq_y)(k_y' - gq_y + q_y) - v_f^2 k_z'^2}{\left[(k_n + iv_t k_y')^2 + v_f^2|\mathbf{k}'|^2 + \left(v_f^2 - v_t^2\right)g(1-g)q_y^2\right]^2} \\
&= J_c \int e^{iq_y R_y} dq_y \int dk_x \int dk_y' \int dk_n \int_0^1 dg \frac{-\pi\left\{2k_n^2 + ik_n(4k_y' + q_y - 2gq_y)v_t + k_y'(2k_y' + q_y - 2gq_y)\left(v_f^2 - v_t^2\right)\right\}}{2v_f\left\{(k_n + iv_t k_y')^2 + v_f^2 k_x^2 + v_f^2 k_y'^2 + \left(v_f^2 - v_t^2\right)g(1-g)q_y^2\right\}^{\frac{3}{2}}} \\
&= J_c \int dk_x \int dk_y' \int dk_n \int_{-\infty}^{\infty} dq_y e^{iq_y R_y} \frac{\left[v_f^2\left(k_x^2 + k_y'^2\right) - (ik_n - v_t k_y')^2\right]^{-\frac{1}{2}}\left[4\pi v_f^2 k_y'^2 - 4\pi(ik_n - v_t k_y)^2\right]}{v_f\left[4(ik_n - v_t k_y')^2 - 4v_f^2\left(k_x^2 + k_y'^2\right) - \left(v_f^2 - v_t^2\right)q_y^2\right]} \\
&= J_c \int_{-\infty}^{\infty} dk_x \int_{-\infty}^{\infty} dk_y' \int_{-\infty}^{\infty} dk_n \frac{e^{-2R_y\sqrt{\frac{v_f^2(k_x^2+k_y'^2)-(ik_n - v_t k_y')^2}{v_f^2 - v_t^2}}} 2\pi^2\left[(ik_n - v_t k_y')^2 - v_f^2 k_y'^2\right]}{v_f\sqrt{v_f^2 - v_t^2}\left[v_f^2\left(k_x^2 + k_y'^2\right) - (ik_n - v_t k_y')^2\right]} \\
&= J_c \int_0^{\infty} k^2 dk \int_0^{\pi} \sin\theta d\theta \int_0^{2\pi} d\varphi \frac{e^{-2R_y k\sqrt{\frac{\sin^2(\theta) - \left[i\cos(\theta) - \frac{v_t \sin(\theta)\sin(\varphi)}{v_f}\right]^2}{v_f^2 - v_t^2}}} 2\pi^2\left\{\left[i\cos(\theta) - \frac{v_t \sin(\theta)\sin(\varphi)}{v_f}\right]^2 - \left[\sin(\theta)\sin(\varphi)\right]^2\right\}}{v_f^3\sqrt{v_f^2 - v_t^2}\left\{\sin^2(\theta) - \left[i\cos(\theta) - \frac{v_t \sin(\theta)\sin(\varphi)}{v_f}\right]^2\right\}} \\
&= J_c \int_0^{\pi} d\theta \int_0^{2\pi} d\varphi \frac{-\pi^2 \sin(\theta)\left\{\sin^2(\theta)\sin^2(\varphi) + \left[\cos(\theta) + \frac{iv_t \sin(\theta)\sin(\varphi)}{v_f}\right]^2\right\}}{2R_y^3 v_f^3\left(v_f^2 - v_t^2\right)^{-1}\left\{\sin^2(\theta) + \left[\cos(\theta) + \frac{iv_t \sin(\theta)\sin(\varphi)}{v_f}\right]^2\right\}^{5/2}} \\
&= J_c \int_0^{2\pi} d\varphi \frac{\pi^2\left(v_f^2 - v_t^2\right)[-2 + \cos(2\varphi)]}{3v_f^3 R_y^3} \\
&= -\frac{4\pi^3 J_c}{3v_f}\frac{\left(1 - v_t^2/v_f^2\right)}{R_y^3}.
\end{aligned} \tag{B3}$$

Following the similar process, one can obtain

$$J_x(R_y) = J_z(R_y),$$
$$J_y(R_y) = \frac{4\pi^3 J_c}{3v_f^3}\frac{v_t^2}{R_y^3},$$
$$J_y^{DM}(R_y) = 0. \tag{B4}$$

Noting that the interlayer RKKY interaction here can be modified by the tilt parameter v_t. This is attributed to the tilt-dependent energy difference [51] $E_{+,\lambda}(k_y, k_\parallel) - E_{-,\lambda}(k_y + q_y, k_\parallel)$ [Eq. (2) of the main text], where the transferred momentum q_y couples tightly with v_t.

APPENDIX C: INTERLAYER RKKY INTERACTION WITH FMS STACKED IN THE z AXIS

For the arrangement of FMs with their stacking direction parallel to the z axis, i.e., $k_\perp = k_z$ and $\mathbf{k}_\parallel = (k_x, k_y)$. Utilizing Eqs. (2), (3), and (7) in the main text, the Matsubara Green's function $G^\lambda_{k_z+q_z,\mathbf{k}_\parallel}(ik_n)$ of $u_F = 0$ can be constructed as

$$G^\lambda_{k_z+q_z,\mathbf{k}_\parallel}(ik_n) = \frac{ik_n - v_t k_y + H_0(k_z+q_z, \mathbf{k}_\parallel)}{(ik_n - v_t k_y)^2 - \varepsilon^2(k_z+q_z, \mathbf{k}_\parallel)} \tag{C1}$$

Unlike the two cases in previous sections, the interlayer RKKY interaction here include intravalley and intervalley contributions, i.e., $\lambda = \lambda'$ and $\lambda \neq \lambda'$ coexist at the same time in the Eq. (6) of the main text. Under this consideration, one can use the Eq. (C1) and Eqs. (5)–(6) of the main text to simplify the interlayer RKKY interaction $J(R_z)$ as

$$J(R_z) = \sum_{\alpha=x,y,z} J_\alpha(R_z) S_\alpha^T S_\alpha^B + J_{fr}(R_z)\left(S_y^T S_z^B + S_z^T S_y^B\right), \tag{C2}$$

with

$$\frac{J_x(R_z)}{J_c} = \sum_{\lambda,\lambda'}\int_{-\infty}^{\infty} dq_z' e^{iq_z' R_z}\int_{-\infty}^{\infty} d\mathbf{k}'\int_{-\infty}^{\infty} dk_n \int_0^1 dg \frac{(ik_n - v_t k_y)^2 + v_f^2\left(k_x^2 - k_y^2\right) - \lambda\lambda' v_f^2 (k_z' - gq_z')(k_z' + q_z' - gq_z')}{2e^{-i(\lambda'-\lambda)QR_z}\left[(k_n + iv_t k_y)^2 + v_f^2|\mathbf{k}'|^2 + g(1-g)v_f^2 q_z'^2\right]^2},$$
$$\frac{J_y(R_z)}{J_c} = \sum_{\lambda,\lambda'}\int_{-\infty}^{\infty} dq_z' e^{iq_z' R_z}\int_{-\infty}^{\infty} d\mathbf{k}'\int_{-\infty}^{\infty} dk_n \int_0^1 dg \frac{(ik_n - v_t k_y)^2 - v_f^2\left(k_x^2 - k_y^2\right) - \lambda\lambda' v_f^2 (k_z' - gq_z')(k_z' + q_z' - gq_z')}{2e^{-i(\lambda'-\lambda)QR_z}\left[(k_n + iv_t k_y)^2 + v_f^2|\mathbf{k}'|^2 + g(1-g)v_f^2 q_z'^2\right]^2},$$
$$\frac{J_z(R_z)}{J_c} = \sum_{\lambda,\lambda'}\int_{-\infty}^{\infty} dq_z' e^{iq_z' R_z}\int_{-\infty}^{\infty} d\mathbf{k}'\int_{-\infty}^{\infty} dk_n \int_0^1 dg \frac{(ik_n - v_t k_y)^2 - v_f^2\left(k_x^2 + k_y^2\right) + \lambda\lambda' v_f^2 (k_z' - gq_z')(k_z' + q_z' - gq_z')}{2e^{-i(\lambda'-\lambda)QR_z}\left[(k_n + iv_t k_y)^2 + v_f^2|\mathbf{k}'|^2 + g(1-g)v_f^2 q_z'^2\right]^2},$$
$$\frac{J_{fr}(R_z)}{J_c} = \sum_{\lambda,\lambda'}\int_{-\infty}^{\infty} dq_z' e^{iq_z' R_z}\int_{-\infty}^{\infty} d\mathbf{k}'\int_{-\infty}^{\infty} dk_n \int_0^1 dg \frac{v_f^2 k_y[(\lambda+\lambda')k_z' + q_z'(\lambda' - g(\lambda+\lambda'))]}{2e^{-i(\lambda'-\lambda)QR_z}\left[(k_n + iv_t k_y)^2 + v_f^2|\mathbf{k}'|^2 + g(1-g)v_f^2 q_z'^2\right]^2},$$

where $\mathbf{k}' = (k_x, k_y, k_z')$, the Feynman parametrization is similar to the Eq. (A4) and the coordinate transformation $(q_z + \lambda Q - \lambda' Q, k_z - \lambda Q + gq_z') = (q_z', k_z')$ are used. Here, the DM term always vanishes due to the protected inversion symmetry of the Green's function, i.e., $G(R_z, ik_n) = G(-R_z, ik_n)$ with $G(\pm R_z, ik_n) = \sum_{k_z,\mathbf{k}_\parallel,\lambda} e^{\pm ik_z R_z} G^\lambda_{k_z,\mathbf{k}_\parallel}(ik_n)$. Similar result has also been found for the RKKY interaction of magnetic impurities in WSMs [46].

Taking the component $J_x(R_z)$ as an example, whose detailed calculation process is given by

$$\begin{aligned}
\frac{J_x(R_z)}{J_c} &= \sum_{\lambda,\lambda'}\int_{-\infty}^{\infty} dq_z' e^{iq_z' R_z}\int_0^1 dg\int_{-\infty}^{\infty} d\mathbf{k}'\int_{-\infty}^{\infty} dk_n \frac{(ik_n - v_t k_y)^2 + v_f^2\left(k_x^2 - k_y^2\right) - \lambda\lambda' v_f^2 (k_z' - gq_z')(k_z' + q_z' - gq_z')}{2e^{-i(\lambda'-\lambda)QR_z}\left[(k_n + iv_t k_y)^2 + v_f^2|\mathbf{k}'|^2 + g(1-g)v_f^2 q_z'^2\right]^2} \\
&= \sum_{\lambda,\lambda'}\int dq_z' e^{iq_z' R_z}\int dk_x\int dk_y\int dk_n\int_0^1 dg \frac{\pi\left[(ik_n - v_t k_y)^2(1+\lambda\lambda') - v_f^2\left(k_y^2 - k_x^2\right) - \lambda\lambda' v_f^2\left(k_x^2 + k_y^2\right)\right]}{4e^{-i(\lambda'-\lambda)QR_z} v_f\left[v_f^2\left(k_x^2 + k_y^2\right) + v_f^2 g(1-g)q_z'^2 - (ik_n - v_t k_y)^2\right]^{\frac{3}{2}}} \\
&= \sum_{\lambda,\lambda'}\int dk_x\int dk_y\int dk_n\int_{-\infty}^{\infty} dq_z' \frac{e^{i(q_z+\lambda' Q-\lambda Q)R_z}\pi\left[(ik_n - v_t k_y)^2(1+\lambda\lambda') - v_f^2\left(k_y^2 - k_x^2\right) - \lambda\lambda' v_f^2\left(k_x^2 + k_y^2\right)\right]}{4v_f\sqrt{v_f^2\left(k_x^2 + k_y^2\right) - (ik_n - v_t k_y)^2}\left[v_f^2\left(k_x^2 + k_y^2\right) + \frac{v_f^2 q_z'^2}{4} - (ik_n - v_t k_y)^2\right]} \\
&= \sum_{\lambda,\lambda'}\int_{-\infty}^{\infty} dk_x\int_{-\infty}^{\infty} dk_y\int_{-\infty}^{\infty} dk_n \frac{\pi^2\left[(ik_n - v_t k_y)^2(1+\lambda\lambda') + v_f^2\left(k_x^2 - k_y^2\right) - \lambda\lambda' v_f^2\left(k_x^2 + k_y^2\right)\right]}{2v_f^2 e^{2R_z\sqrt{\frac{v_f^2(k_x^2+k_y^2) - (ik_n - v_t k_y)^2}{v_f^2}} - i(\lambda'-\lambda)QR_z}\left[v_f^2\left(k_x^2 + k_y^2\right) - (ik_n - v_t k_y)^2\right]} \\
&= \sum_{\lambda,\lambda'}\int_0^\infty k^2 dk\int_0^\pi \sin\theta d\theta\int_0^{2\pi} d\varphi \frac{e^{-2R_z k\sqrt{\frac{\sin^2(\theta) - [i\cos(\theta) - \frac{v_t\sin(\theta)\sin(\varphi)}{v_f}]^2}{v_f^2}}}\pi^2\left[i\cos(\theta) - \frac{v_t\sin(\theta)\sin(\varphi)}{v_f}\right]^2}{2e^{-i(\lambda'-\lambda)QR_z} v_f^4\left\{\sin^2(\theta) - \left[i\cos(\theta) - \frac{v_t\sin(\theta)\sin(\varphi)}{v_f}\right]^2\right\}(1+\lambda\lambda')^{-1}}
\end{aligned}$$

$$
\begin{aligned}
&+\sum_{\lambda,\lambda'}\int_0^{\infty}k^2dk\int_0^{\pi}\sin\theta d\theta\int_0^{2\pi}d\varphi\frac{e^{-2R_zk\sqrt{\frac{\sin^2(\theta)-\left[i\cos(\theta)-\frac{v_t\sin(\theta)\sin(\varphi)}{v_f}\right]^2}{v_f^2}}}[\cos(2\varphi)-\lambda\lambda']\pi^2\sin^2(\theta)}{2e^{-i(\lambda'-\lambda)QR_z}v_f^4\left\{\sin^2(\theta)-\left[i\cos(\theta)-\frac{v_t\sin(\theta)\sin(\varphi)}{v_f}\right]^2\right\}}\\
&=\sum_{\lambda,\lambda'}\int_0^{\pi}d\theta\int_0^{2\pi}d\varphi\frac{\pi^2\left\{[\cos(2\varphi)-\lambda'\lambda]\sin^2(\theta)+(1+\lambda'\lambda)\left[\cos(\theta)+\frac{iv_t\sin(\theta)\sin(\varphi)}{v_f}\right]^2\right\}}{8v_fR_z^3\left\{\sin^2(\theta)+\left[\cos(\theta)+\frac{iv_t\sin(\theta)\sin(\varphi)}{v_f}\right]^2\right\}^{\frac{5}{2}}e^{-i(\lambda'-\lambda)QR_z}\sin^{-1}(\theta)}\\
&=\sum_{\lambda,\lambda'}\int_0^{2\pi}d\varphi\frac{\pi^2[2\cos(2\varphi)-3\lambda\lambda'-1]}{12v_fR_z^3}e^{i(\lambda'-\lambda)QR_z}\\
&=\sum_{\lambda,\lambda'}\frac{-\pi^3(1+3\lambda\lambda')}{6v_fR_z^3}e^{i(\lambda'-\lambda)QR_z}\\
&=\frac{2\pi^3}{3v_f}\frac{\cos(2QR_z)-2}{R_z^3}.
\end{aligned}
\tag{C3}
$$

Performing some similar algebraic calculations, other RKKY components can be easily solved as

$$
J_y(R_z)=J_x(R_z)\quad J_z(R_z)=\sum_{\lambda,\lambda'}\frac{\pi^3(\lambda\lambda'-1)J_c}{6v_fR_z^3}e^{i(\lambda'-\lambda)QR_z}=-\frac{2\pi^3J_c}{3v_f}\frac{\cos(2QR_z)}{R_z^3},\quad J_{fr}(R_z)=0. \tag{C4}
$$

In contrast with the components $J_\alpha(R_{x,y})$, there aries an extra oscillation $\cos(2QR_z)$ for $J_\alpha(R_z)$, which is induced by the separated projections of Weyl points in the k_z axis, similar to the RKKY interaction of magnetic impurities in WSMs [45,46]. Here, the response of the RKKY components ($u_F=0$) to the tilting parameter v_t is similar to the case of Appendix A, i.e., the v_t-related terms are completely eliminated in the energy difference $E_{+,\lambda}(k_z,k_\parallel)-E_{-,\lambda}(k_z+q_z,k_\parallel)$, which naturally leads to v_t-independent RKKY components [Eq. (C3) and Eq. (C4)].

[1] G. Chang, S.-Y. Xu, B. J. Wieder, D. S. Sanchez, S.-M. Huang, I. Belopolski, T.-R. Chang, S. Zhang, A. Bansil, H. Lin, and M. Z. Hasan, Phys. Rev. Lett. **119**, 206401 (2017).

[2] Y. Wu, D. Mou, N. H. Jo, K. Sun, L. Huang, S. L. Bud'ko, P. C. Canfield, and A. Kaminski, Phys. Rev. B **94**, 121113(R) (2016).

[3] P. Hosur, Phys. Rev. B **86**, 195102 (2012).

[4] D. Ma, H. Chen, H. Liu, and X. C. Xie, Phys. Rev. B **97**, 045148 (2018).

[5] Y. Zheng, W. Chen, and D. Y. Xing, Phys. Rev. B **104**, 075420 (2021).

[6] A. A. Zyuzin, S. Wu, and A. A. Burkov, Phys. Rev. B **85**, 165110 (2012).

[7] I. A. Shojaei, S. Pournia, C. Le, B. R. Ortiz, G. Jnawali, F.-C. Zhang, S. D. Wilson, H. E. Jackson, and L. M. Smith, Sci. Rep. **11**, 8155 (2021).

[8] J. Y. Liu, J. Hu, Q. Zhang, D. Graf, H. B. Cao, S. M. A. Radmanesh, D. J. Adams, Y. L. Zhu, G. F. Cheng, X. Liu, W. A. Phelan, J. Wei, M. Jaime, F. Balakirev, D. A. Tennant, J. F. DiTusa, I. Chiorescu, L. Spinu, and Z. Q. Mao, Nature Mater. **16**, 905 (2017).

[9] X. S. Li, C. Wang, M. X. Deng, H. J. Duan, P. H. Fu, R. Q. Wang, L. Sheng, and D. Y. Xing, Phys. Rev. Lett. **123**, 206601 (2019).

[10] S.-Y. Xu, I. Belopolski, D. S. Sanchez, C. Zhang, G. Chang, C. Guo, G. Bian, Z. Yuan, H. Lu, T.-R. Chang, P. P. Shibayev, M. L. Prokopovych, N. Alidoust, H. Zheng, C.-C. Lee, S.-M. Huang, R. Sankar, F. Chou, C.-H. Hsu, H.-T. Jeng, A. Bansil, T. Neupert, V. N. Strocov, H. Lin, S. Jia, and M. Z. Hasan, Sci. Adv. **1**, e1501092 (2015).

[11] C. Shekhar, A. K. Nayak, Y. Sun, M. Schmidt, M. Nicklas, I. Leermakers, U. Zeitler, Y. Skourski, J. Wosnitza, Z. Liu, Y. Chen, W. Schnelle, H. Borrmann, Y. Grin, C. Felser, and B. Yan, Nature Phys. **11**, 645 (2015).

[12] S.-Y. Xu, N. Alidoust, I. Belopolski, Z. Yuan, G. Bian, T.-R. Chang, H. Zheng, V. N. Strocov, D. S. Sanchez, G. Chang, C. Zhang, D. Mou, Y. Wu, L. Huang, C.-C. Lee, S.-M. Huang, B. Wang, A. Bansil, H.-T. Jeng, T. Neupert *et al.*, Nature Phys. **11**, 748 (2015).

[13] Y. Zhou, P. Lu, Y. Du, X. Zhu, G. Zhang, R. Zhang, D. Shao, X. Chen, X. Wang, M. Tian, J. Sun, X. Wan, Z. Yang, W. Yang, Y. Zhang, and D. Xing, Phys. Rev. Lett. **117**, 146402 (2016).

[14] S.-M. Huang, S.-Y. Xu, I. Belopolski, C.-C. Lee, G. Chang, B. Wang, N. Alidoust, G. Bian, M. Neupane, C. Zhang, S. Jia, A. Bansil, H. Lin, and M. Z. Hasan, Nature Commun. **6**, 7373 (2015).

[15] B. Q. Lv, H. M. Weng, B. B. Fu, X. P. Wang, H. Miao, J. Ma, P. Richard, X. C. Huang, L. X. Zhao, G. F. Chen, Z. Fang, X. Dai, T. Qian, and H. Ding, Phys. Rev. X **5**, 031013 (2015).

[16] G. Xu, H. Weng, Z. Wang, X. Dai, and Z. Fang, Phys. Rev. Lett. **107**, 186806 (2011).

[17] X. Wan, A. M. Turner, A. Vishwanath, and S. Y. Savrasov, Phys. Rev. B **83**, 205101 (2011).

[18] E. Liu, Y. Sun, N. Kumar, L. Muechler, A. Sun, L. Jiao, S.-Y. Yang, D. Liu, A. Liang, Q. Xu, J. Kroder, V. Süß, H. Borrmann, C. Shekhar, Z. Wang, C. Xi, W. Wang, W. Schnelle, S. Wirth,

Y. Chen, S. T. B. Goennenwein *et al.*, Nature Phys. **14**, 1125 (2018).
[19] J. Kübler and C. Felser, Europhys. Lett. **114**, 47005 (2016).
[20] Z. Wang, M. G. Vergniory, S. Kushwaha, M. Hirschberger, E. V. Chulkov, A. Ernst, N. P. Ong, R. J. Cava, and B. A. Bernevig, Phys. Rev. Lett. **117**, 236401 (2016).
[21] D. F. Liu, A. J. Liang, E. K. Liu, Q. N. Xu, Y. W. Li, C. Chen, D. Pei, W. J. Shi, S. K. Mo, P. Dudin, T. Kim, C. Cacho, G. Li, Y. Sun, L. X. Yang, Z. K. Liu, S. S. P. Parkin, C. Felser, and Y. L. Chen, Science **365**, 1282 (2019).
[22] A. A. Soluyanov, D. Gresch, Z. Wang, Q. Wu, M. Troyer, X. Dai, and B. A. Bernevig, Nature (London) **527**, 495 (2015).
[23] G. Sharma, P. Goswami, and S. Tewari, Phys. Rev. B **93**, 035116 (2016).
[24] A. Menon, D. Chowdhury, and B. Basu, Phys. Rev. B **98**, 205109 (2018).
[25] D. Ma, H. Jiang, H. Liu, and X. C. Xie, Phys. Rev. B **99**, 115121 (2019).
[26] S. H. Zheng, H. J. Duan, J. K. Wang, J. Y. Li, M. X. Deng, and R. Q. Wang, Phys. Rev. B **101**, 041408(R) (2020).
[27] W. Rao, Y. L. Zhou, Y. J. Wu, H. J. Duan, M. X. Deng, and R. Q. Wang, Phys. Rev. B **103**, 155415 (2021).
[28] J. Shao and L. Yan, J. Phys.: Condens. Matter **33**, 185704 (2021).
[29] M. X. Deng, G. Y. Qi, R. Ma, R. shen, R. Q. Wang, L. Sheng, an D. Y. Xing, Phys. Rev. Lett. **122**, 036601 (2019).
[30] D. Sinha, Phys. Rev. B **102**, 085144 (2020).
[31] C.-Y. Zhu, W.-H. Xu, Y.-L. Zhou, J.-Y. Ba, M.-X. Deng, H.-J. Duan, and R.-Q. Wang, Phys. Rev. B **103**, 075148 (2021).
[32] C.-Y. Zhu, S.-H. Zheng, H.-J. Duan, M.-X. Deng, H.-J. Duan, and R.-Q. Wang, Front. Phys. **15**, 23602 (2020).
[33] M. A. Ruderman and C. Kittel, Phys. Rev. **96**, 99 (1954).
[34] T. Kasuya, Prog. Theor. Phys. **16**, 45 (1956).
[35] K. Yosida, Phys. Rev. **106**, 893 (1957).
[36] D. A. Abanin and D. A. Pesin, Phys. Rev. Lett. **106**, 136802 (2011).
[37] J.-J. Zhu, D.-X. Yao, S.-C. Zhang, and K. Chang, Phys. Rev. Lett. **106**, 097201 (2011).
[38] V. Kaladzhyan, A. A. Zyuzin, and P. Simon, Phys. Rev. B **99**, 165302 (2019).
[39] V. D. Kurilovich, P. D. Kurilovich, and I. S. Burmistrov, Phys. Rev. B **95**, 115430 (2017).
[40] S. K. Firoz Islam, P. Dutta, A. M. Jayannavar, and A. Saha, Phys. Rev. B **97**, 235424 (2018).
[41] H.-J. Duan, S.-H. Zheng, P.-H. Fu, R.-Q. Wang, J.-F. Liu, G.-H. Wang, and M. Yang, New J. Phys. **20**, 103008 (2018).
[42] M. Zare, F. Parhizgar, and R. Asgari, Phys. Rev. B **94**, 045443 (2016).
[43] H.-J. Duan, S.-H. Zheng, Y.-Y. Yang, C.-Y. Zhu, M.-X. Deng, M. Yang, and R.-Q. Wang, Phys. Rev. B **102**, 165110 (2020).
[44] M. Shiranzaei, H. Cheraghchi, and F. Parhizgar, Phys. Rev. B **96**, 024413 (2017).
[45] H.-R. Chang, J. Zhou, S.-X. Wang, W.-Y. Shan, and D. Xiao, Phys. Rev. B **92**, 241103(R) (2015).
[46] M. V. Hosseini and M. Askari, Phys. Rev. B **92**, 224435 (2015).
[47] P. Bruno and C. Chappert, Phys. Rev. Lett. **67**, 1602 (1991).
[48] P. Bruno and C. Chappert, Phys. Rev. B **46**, 261 (1992).
[49] M. Li, W. Cui, J. Yu, Z. Dai, Z. Wang, F. Katmis, W. Guo, and J. Moodera, Phys. Rev. B **91**, 014427 (2015).
[50] C. S. Ho and M. B. A. Jalil, AIP Adv. **7**, 055926 (2017).
[51] M. M. Asmar and W.-K. Tse, Phys. Rev. B **100**, 014410 (2019).
[52] H.-J. Duan, S.-H. Zheng, R.-Q. Wang, M.-X. Deng, and M. Yang, Phys. Rev. B **99**, 165111 (2019).
[53] A. A. Zyuzin and R. P. Tiwari, JETP Lett. **103**, 717 (2016).
[54] B. Khodadadi, J. B. Mohammadi, J. M. Jones, A. Srivastava, C. Mewes, T. Mewes, and C. Kaiser, Phys. Rev. Appl. **8**, 014024 (2017).
[55] P. A. A. van der Heijden, P. J. H. Bloemen, and J. M. Metselaar, R. M. Wolf, J. M. Gaines, J. T. W. M. vanEemeren, P. J. van der Zaag, and W. J. M. de Jonge, Phys. Rev. B **55**, 11569 (1997).
[56] S. Kaneta-Takada, Y. K. Wakabayashi, Y. Krockenberger, S. Ohya, M. Tanaka, Y. Taniyasu, and H. Yamamoto, Appl. Phys. Lett. **118**, 092408 (2021).
[57] Y. K. Wakabayashi, S. Kaneta-Takada, Y. Krockenberger, K. Takiguchi, S. Ohya, M. Tanaka, Y. Taniyasu, and H. Yamamoto, AIP Adv. **11**, 035226 (2021).
[58] Z. Wang, Y. Sun, X.-Q. Chen, C. Franchini, G. Xu, H. Weng, X. Dai, and Z. Fang, Phys. Rev. B **85**, 195320 (2012).
[59] C.-X. Liu, B. Roy, and J. D. Sau, Phys. Rev. B **94**, 235421 (2016).
[60] R. Okugawa and S. Murakami, Phys. Rev. B **89**, 235315 (2014).
[61] L. Yang, L. Jin, L. Wysocki, J. Schöpf, D. Jansen, B. Das, L. Kornblum, P. H. M. van Loosdrecht, and I. Lindfors-Vrejoiu, Phys. Rev. B **104**, 064444 (2021).